Politecnico di Torino

Master's Degree in Automotive Engineering

Academic Year 2020/2021

Graduation session on July 2021

Drowsiness detection levels

Design and analysis of drowsy driver model

Supervisor:

prof. Daniela Misul

Candidate:

Simone Todaro

Tutor:

Eng. Alberto Bertone

To the little ones:
Marco, Alessio,
Nicolò, Arianna,
& Mattia

And to the older ones:
Nonna Vi
&
Nonno
who is
celebrating
from the sky

Abstract

This thesis deals with the study and simulation of methods to identify levels of drowsiness in drivers of motor vehicles for the period of prolonged driving.

Fatigue and distraction are the cause of a large number of road accidents in the world. The causes of high fatigue during driving are mainly: lack of rest, excessive driving times, travel at night and weariness in general. The vast majority of drivers do not recognize or underestimate the limitations of the ability to react due to fatigue. In fact, generally you continue the journey despite the arrival of clear symptoms of tiredness. Development of driving aids is of current interest in order to reduce critical situation. Specifically for the drowsiness, the aim is to warn the driver in time during travel, recognizing his degree of fatigue in advance.

In this document, in addition to an overall view of the existing techniques for identifying the drowsiness, it is presented a drowsiness model able to replicate different drowsy drivers according to their level of sleepiness.

The main objective was the study and design of the driver model, simulating at the end the effective trajectory covered by the different car users in a standardized double lane change manoeuvre and in a longer open track.

Contents

List of figure

List of symbols

a	distance between centre of mass and front axle
b	distance between centre of mass and rear axle
d	distance
g	acceleration of gravity
h_G	height of the centre of mass on the road
k	stiffness
l	wheelbase
L	predictive distance
m	mass
m_s	sprung mass
m_u	unsprung mass
t	time
u, v, w	components of the velocity along x, y and z axes
$\dot{u}, \dot{v}, \dot{w}$	derivative of the components of the velocity along x, y and z axes
$\{z\}$	state vector
$[A]$	dynamic matrix
$[B]$	input gain matrix
C	cornering stiffness
C_y	drag coefficient
F	force
F_c	centrifugal force
G	centre of mass
J	mass moment of inertia
M	torque
M_z	aligning moment
$Gxyz$	vehicle reference frame
$OXYZ$	inertial reference frame
R	radius of the trajectory
S	projection area

V	vehicle speed
α	sideslip angle of the tire
β	sideslip angle of the vehicle
$\dot{\beta}$	derivative of the sideslip angle of the vehicle
δ	steering angle
ρ	density of air
τ	time delay
φ	roll angle
χ	torsional stiffness
ψ	yaw angle
$\dot{\psi}, r$	yaw rate

Introduction

The carelessness of the driver is considered one of the major causes of car accidents on motorways. The National Highway Traffic Safety Administration (NHTSA) estimates that nearly 25% of reported accidents by the police are due to some form of inattention: the driver is distracted, asleep or is stressed [1].

There are different types of fatigue depending on the specific functionalities involved: local physical exhaustion, general physical exhaustion, central nervous and mental fatigue. Central nervous and mental fatigue are the types more dangerous for the driver, indeed, usually these types of collapse significantly lead to drowsiness reducing the attention and promptness of the driver in responding to dangerous situations and greatly increasing the probability of an accident.

When a driver is stressed and begins to become drowsy, the following symptoms can be observed: frequent yawns, difficulty in keeping eyes open, confusion, irritability, slower reactions and responses, a sensation of burning in the eyes, difficulty in maintaining concentration, shallow breathing, low heart rate and head or body sway compared to the normal position.

Each person shows different and variable symptoms so that it does not exist a certain and universal method of measuring the level of fatigue.

The ETSC study [2] shows that the level of fatigue or drowsiness is a function of the amount of activity related to the psychological capacity of brain wake.

However, it is generally agreed that three main factors contribute to tiredness: lack of rest, time of day and duration of a particular action. A study [3] showed that 17 hours of continuous waking degrade driving performance in the same way as an alcohol concentration of 0.05% in the blood, which in many countries is still the legal limit.

In addition, the lack of rest over a period of 24 hours is the same as the 0.10% alcohol concentration in the blood.

Another situation is monotonous driving, particularly exhausting and can rapidly lead to a loss of concentration [4].

The typical behaviour of a fatigued driver is the difficulty to keep the vehicle inside the lane, the tendency to leave the road, frequent and not required speed changes and limited ability to react in dangerous situations.

The transition from being fatigued to nodding off is subtle and generally goes unnoticed by the driver. Drivers often ignore the symptoms of fatigue and for this reason, a system of identification of the drowsiness is desirable. In the transport industry for example is particularly useful; it has been shown that 57% of all fatal accidents involving lorries are due to tiredness [5].

Before developing such a system it is important to define the type of fatigue that is going to be detected [6]. Identification methods can be divided into techniques that directly monitor the driver and techniques that monitor the behaviour of the vehicle following the driver's commands.

1. Drowsiness detection methods

Figure 1: Drowsiness detection

Generally, identification methods can be separated into technologies that directly analyse the interior compartment, so the driver and what there is around him and tools that examine the vehicle's behaviour during travel.

1.1 Drowsiness detection based on driver monitoring

1.1.1 Physiological measurement

Techniques that directly monitor the driver include the measurement of physiological conditions (such as brain waves, pulsations, pressure). In the medical world, the electroencephalogram (EEG) has found numerous applications and it begins to be adopted also in a vehicle since it is employed to characterize sleep and for this reason, it is a logical approach to tiredness detection [7]. EEG measurements have the advantage of being very accurate, but the main disadvantage of being intrusive. These signals, in fact, are collected by electrodes connected to the human body.

An EEG-based algorithm for driver fatigue detection was suggested in [8].

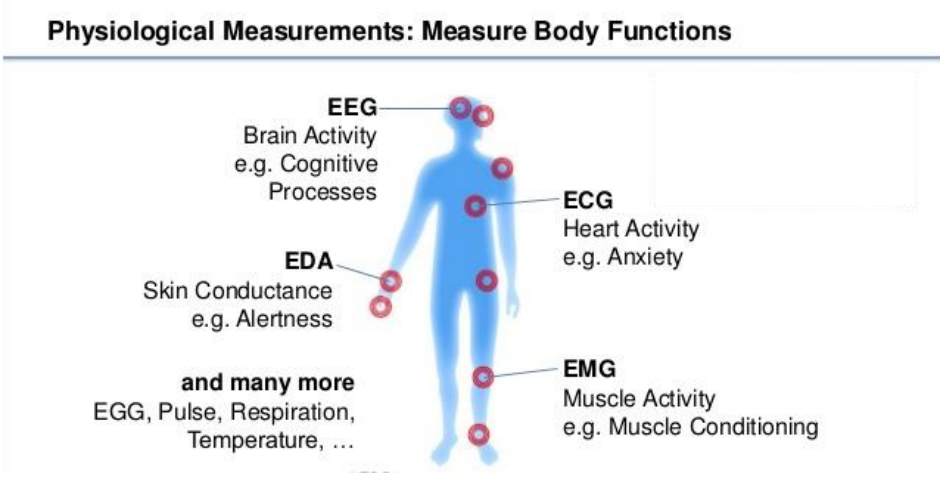

Figure 2: Physiological measurement

In general, all the physiological measurements like brain activity, heart rate, skin conductance, muscle activity allow a better accuracy in terms of identification of the drowsiness, but they are often intrusive methods that involve the use of electrodes and sensors connected to the driver. Due to this, such solutions cause a nuisance to the driver and are impractical in many situations, especially as a market solution. In any case, the physiological measures can be used as a reference in assessing other techniques [9].

1.1.2 Facial recognition

Control eye and eyelid movement using cameras, adopting artificial intelligence, is an established technique for the identification of fatigue, and for this reason, many of the efforts of modern researchers have been focused on the development of such methodologies. The driver monitoring camera embedded with facial recognition verifies the alertness and condition of the driver controlling beyond eyes and eyelids [10] also head movements and expressions like frequent yawning.

Figure 3: Facial recognition

Using a camera to monitor the driver is also not intrusive method since no direct interaction with the devices is required. However, these techniques are sensitive to external factors such as the lighting and appearance of the driver (for example whether or not he wears the glasses).

1.2 Drowsiness detection based on vehicle monitoring

Techniques for monitoring vehicle behaviour analyse physical variables related to the geometry of the vehicle itself and parameters computed onboard as speed of travel, steering wheel angle, steering wheel angle speed, the trajectory and the lateral position concerning the boundaries [11]. These last ones need cameras for lane monitoring and images acquisition.

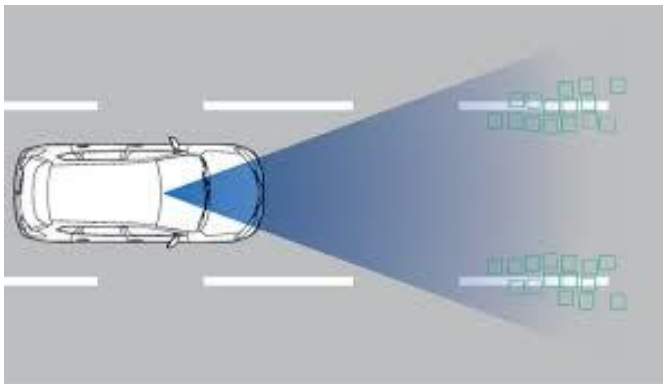

Figure 4: Lane monitoring

Obviously, the lane monitoring system works as long a driver actually steers a vehicle actively instead of an automatic lane-keeping system.

Another more intuitive method for monitoring a subject's driving behaviour is to directly monitor the inputs made to the vehicle's steering wheel. The practical implementation of steering wheel movement monitoring fulfils the requirement for a cost-effective and easy to implement a method for drowsiness detection. It is a pure software solution without the need for additional sensors other than the steering angle sensor. Thus it can easily be integrated into existing vehicle platforms.

In addition as the lane monitoring system they are completely non-invasive techniques for the driver, making them suitable for the practical application, but, on the other hand, have limitations dictated by the subjectivity so the experience of the driver, the driving conditions and the type of vehicle [12].

Figure 5: Steering pattern monitoring

During any journey, drivers provide many steering inputs to guide their vehicles. Decreased concentration and tiredness impair steering behaviour and reduce the driver's reaction time. The typical steering patterns which indicate drowsiness begin to occur well before the driver falls asleep at the wheel.

The majority of sampled drivers tend to show an increasing trend towards faster and larger steering corrections as they become drowsy [13]. Not only the regularity of input decrease in drowsy drivers, but when they occur they are large

and sudden. Steering inputs in fatigued drivers are shown to have fewer micro corrections and more macro-corrections, with sleeping drivers making no corrections [14]. Based on the frequency of these movements and other parameters, among them the length of a trip, use of turn signals, and the time of day, the software calculates the driver's level of fatigue. If that level exceeds a certain value, an icon such as a coffee cup flashes on the instrument panel to warn drivers that they need a rest.

Figure 6: Attention assist

However, detecting a single occurrence of one of these steering patterns is not a clear sign of fatigue. As studies have shown [15] [16], it is only when they become more frequent that increasing drowsiness is apparent. As the occurrence of these steering patterns is different from driver to driver, the driver's steering behaviour is analysed at the start of the journey and individual driving styles are taken into account.

1.2.1 Market solution by Bosch

The initial signs of fatigue can be detected before a critical situation arises. The Bosch driver drowsiness detection can do this by monitoring steering movements and advising drivers to take a break in time.

The system is based on an algorithm, which begins recording the driver's steering behaviour the moment the trip begins. Then it recognizes changes over the course of long trips, and thus also the driver's level of fatigue. Typical signs of waning concentration are phases during which the driver is barely steering, combined with slight, but quick and abrupt steering movements to keep the car on the track.

These phases are a sign of decreased concentration and increased fatigue.

Driver Drowsiness Detection searches for characteristic features in a driver's steering behaviour. The function evaluates data from a high-resolution steering-angle sensor (accuracy <0.1°) or, alternatively, from electric power steering. This information is supplemented by situational parameters such as duration of the journey, the monotony of journey and time of day. By means of the vehicle's CAN bus, approximately 70 signals are evaluated by the function's algorithm to assess the driver's level of drowsiness [17].

The algorithm calculates a drowsiness index from these data. If a defined threshold is exceeded, the function triggers a driver warning. This could be an audible signal or a symbol displayed in the instrument cluster (*figure 6*).

As well as warning the driver, data concerning the tiredness of the driver can be used by other systems in the vehicle. In combination with a navigation system, for example, it is possible to display the next available opportunity to stop or take a rest break.

1.3 Market trend

A market investigation has been done in order to sort a large part of the car makers among the previous different technologies.

Considering the technology available and the market trend, there are different combinations between the systems used to detect drowsiness or distraction. They can be divided in steering pattern monitoring, lane monitoring and face monitoring. In some cases there are also other embedded systems as the eye monitoring only used as comparison and validation of the results or the pedal pressure analysis.

The state-of-the-art is the one with all the solutions matched together.

Physiological measurements, as explained above, are not yet suitable for automotive application due to their invasiveness so they have not been found in the current market among all the car makers.

It is important to underline that all the systems are not suitable in urban environment since they are turned on above 60 km/h more or less and after 10 minutes of travel.

Studying the majority of the car makers 3 main combinations can be provided looking the scheme below.

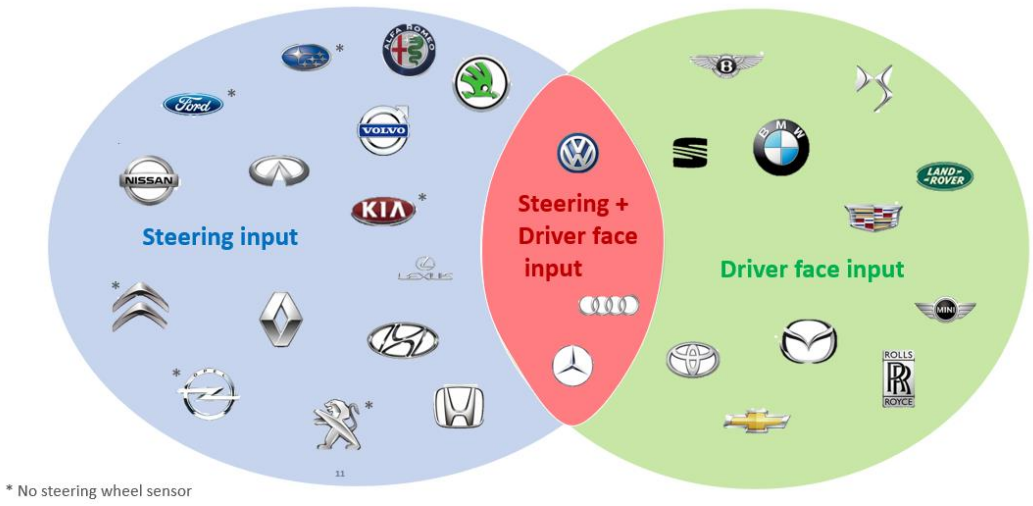

Figure 7: Current market trend

On the left, in blue, the steering pattern monitoring added with the lane monitoring are displayed. It records the driver's steering behaviour and estimates the driver's level of fatigue. It uses algorithms analysing action on the steering wheel (barely, abrupt) based on frequency, length of trip, time of day and lane position. This collection is the biggest, indeed more than half of the brands taken into account are endowed with these tools. Also, for this reason, it is the approach studied and developed in this project. It is important to notice that not all the brands are embedded with steering wheel sensor as specified by the asterisk on the bottom part of the picture.

On the right, in green, the computer vision, always added with the lane monitoring, are shown as the brands that adopt artificial intelligence. In addition, it analyses eyes, eyelids, neck movements using infrared and optical cameras estimating driver's distraction and level of fatigue looking, for example, the occurrence and frequency of the yawns.

In the middle, in red instead, there is the current state of the art in which all the technologies are employed: steering, lane, facial and pedal testing.

Particulars mentioned in appendix A.1.

1.3.1 Car segment involvement

Furthermore, a car segment involvement analysis has been presented in order to verify what are the main vehicle segments involved in the market with driver drowsiness detection systems.

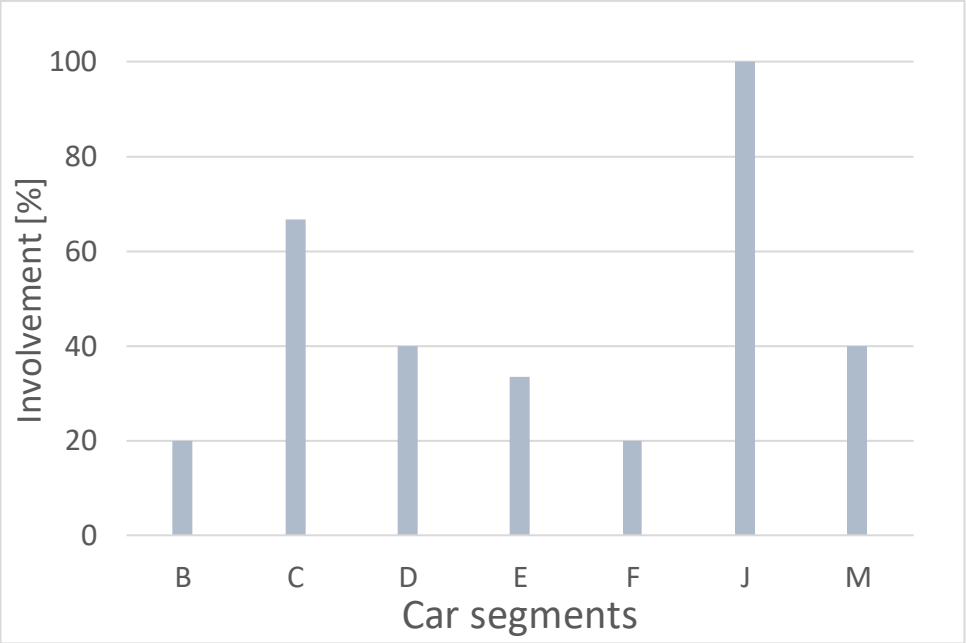

Figure 8: Car segment involvement

Please refer to appendix A.2 for the details. According to the European market taken into account; the SUV segment (included in J) is the one more endowed with tiredness recognition systems, in addition, there are also executive and luxury cars. Basically, all the vehicles beyond a certain price, around more or less 30.000 euros, are embedded with only this solution or suited with other driver assistant systems. There are also some car makers that consider this system as optional and others as included in the price list. Nevertheless, it is becoming a system more and more requested, indeed it should be converted into a mandatory device in all the vehicles sold starting from the year 2022.

2. Vehicle model

The model adopted in this study can be subdivided into two parts joined together: the first one is related to the vehicle representation and the second one associated with the driver. In this chapter, the theory referred to the vehicle model used in the project is explained.

2.1 High speed cornering of a rigid vehicle

In order to avoid extreme simplifications considering an ideal steering system in which all the forces developed at the ground level are equals and are neglected all the external factors; the high-speed cornering model has been chosen to our purpose [18].

2.1.1 Equations of motion

To go further with the simplified model of ideal steering, the distribution of forces between the front and rear axle, the sideslip angle of the vehicle on the path and the sideslip angles of the wheels must be considered.

It is assumed that the vehicle is moving at constant speed on a flat road following a not straight road with a radius R much larger than the wheelbase l so that all sideslip angles, specified as the angles between the speed vector and the longitudinal direction expressed in the local reference frame, are small. The small size of all angles allows the “mono track” or “bicycle” model to be used. This representation, as depicted in the picture below, considers just one wheel for each axle.

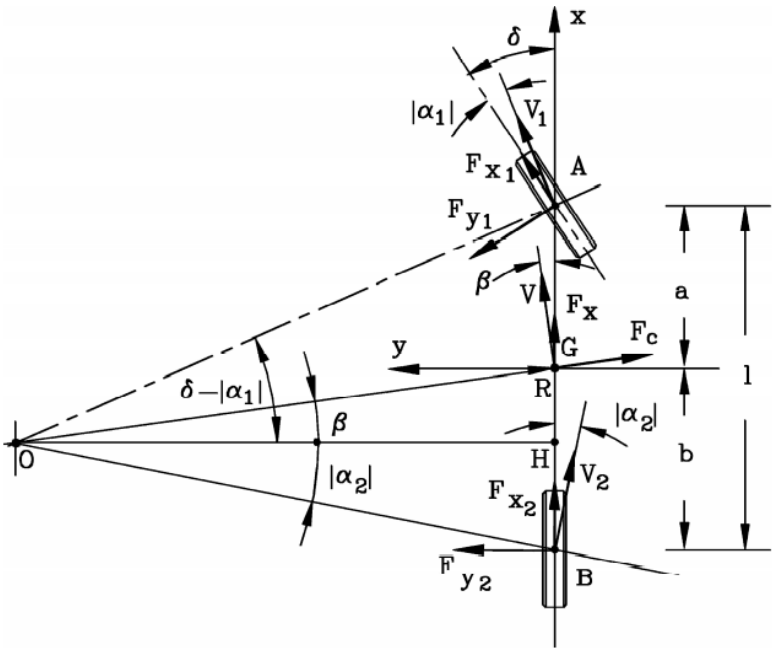

Figure 9: Bicycle model

To keep the model as simple as possible, the car is considered as a rigid body so roll and pitch motion are neglected as well as the vertical displacement due to the suspensions.

The sideslip angle of the vehicle β and of the wheels α are small and also the yaw angular velocity $\dot{\psi}$ can be considered small quantities.

If a motor vehicle is considered as a stiff carcass moving on a surface, a model with three degrees of freedom is needed for the study of its motion.

The motion of the vehicle is described in an inertial reference frame by the X, Ycoordinates of the centre of gravity G of the body and by the yaw angle ψ between the local coordinate x and the global one X. [19]

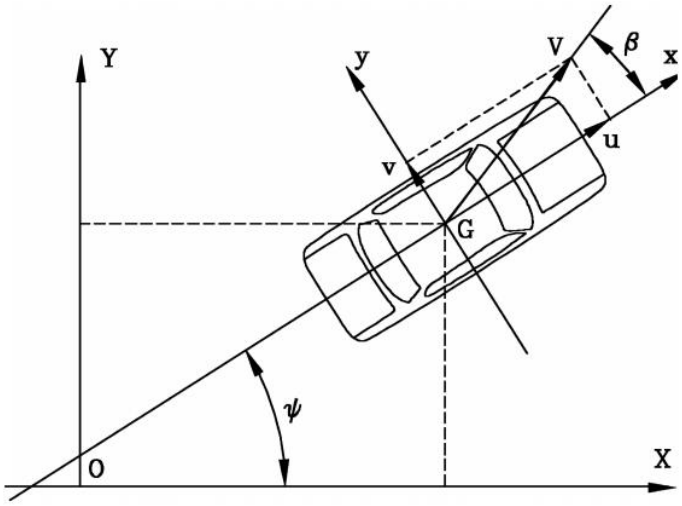

Figure 10: Reference frame of 3 dof model

Hence, the equations of motion of the vehicle are:

$$\begin{cases} m\ddot{X} = F_X \\ m\ddot{Y} = F_Y \\ J_Z\ddot{\psi} = M_Z \end{cases}$$

where F_X, F_Y and M_z are the total forces acting in X and Y directions and the total yawing moment expressed in the inertial reference frame.

It is more convenient to write the equations of motion with respect to the local frame $Gxyz$ since:

- the generalized forces and moments applied to the vehicle $(F_x, F_y, F_z, M_x, M_y, M_z)$ can be written more easily;
- it is possible to linearize the problem (with the exception for ψ) avoiding dealing with trigonometric functions.

This is possible with a simple rotation matrix considering the vector components of the speed u and v in the directions of the x and y axes and the yaw angular velocity $\dot{\psi} = r$:

$$\begin{Bmatrix} F_X \\ F_Y \end{Bmatrix} = \begin{bmatrix} \cos(\psi) & -\sin(\psi) \\ \sin(\psi) & \cos(\psi) \end{bmatrix} \begin{Bmatrix} F_x \\ F_y \end{Bmatrix}$$

Accordingly:

$$\begin{Bmatrix}\dot{X}\\ \dot{Y}\end{Bmatrix} = \begin{bmatrix}\cos(\psi) & -\sin(\psi)\\ \sin(\psi) & \cos(\psi)\end{bmatrix}\begin{Bmatrix}u\\ v\end{Bmatrix}$$

At the end, replacing the terms with the purpose of having all the equations written in the body fixed frame, the system below is achieved:

$$\begin{cases} m(\dot{u} - rv) = F_x \\ m(\dot{v} + rv) = F_y \\ J_z\dot{r} = M_z \end{cases}$$

2.1.2 Linearized handling model

These last equations are non-linear in the velocities u, v, r and the source of nonlinearities are mainly three: the presence of products of these parameters, the presence of trigonometric functions and the nonlinear nature of the forces due to the tires.

However, the linearization is possible if the steering angle δ, the side slip angle of the wheels α and the side slip angle of the vehicle β are small. Such conditions usually are valid for normal driving as in this project when the vehicle is driven far from the limit performances.

So the components of velocity V can be written as:

$$\begin{cases} u = V\cos(\beta) \approx V \\ v = V\sin(\beta) \approx V\beta \end{cases}$$

Considering that v is known it is possible to adapt the previous system of equations:

$$\begin{cases} m\dot{V} = F_x \\ m(\dot{v} + rV) = F_y \\ J_z\dot{r} = M_z \end{cases}$$

If the interaction between longitudinal and transversal forces due to the tires is unattended, the first equation of motion referred to the longitudinal performance

of the vehicle can be uncoupled from the other two. This means that the lateral behaviour is uncoupled from the longitudinal behaviour and it can be described by the unknown variables v and r :

$$\begin{cases} m\,(\dot{v} + rV) = F_y \\ J_z\dot{r} = M_z \end{cases}$$

Or β and r :

$$\begin{cases} mV\left(\dot{\beta} + r\right) + m\beta\dot{V} = F_y \\ J_z\dot{r} = M_z \end{cases}$$

2.1.3 Linearized side slip angles of the wheels

As mentioned before, also the side slipe angle of the wheels need to be small in order to apply the linearization. In this case, at the beginning the relation is:

$$\alpha_i = \beta_i - \delta_i = arctan\left(\frac{v + \dot{\psi}x_i}{u - \dot{\psi}y_i}\right) = arctan\left(\frac{V\beta + \dot{\psi}x_i}{V - \dot{\psi}y_i}\right)$$

The suffix indicates each axle. Then noting that the speed V is the predominant term on the denominator:

$$\begin{cases} \alpha_1 = \beta + \dfrac{a}{V}r - \delta_1 \\ \alpha_2 = \beta - \dfrac{b}{V}r \end{cases}$$

Where the suffix 1 indicates the front, and 2 the rear axis. Eliminating the terms on the denominator, the equations of motion and the side slip forces are referred only to the axles and not to the single tires [20], unanimously with the assumption of the bicycle model.

2.1.4 Forces and moments applied on the vehicle

When lateral accelerations are present, forces on the ground level are exerted. Although with the linearization and neglecting the longitudinal contribution, the total lateral effect is described by the cornering forces, the aerodynamic ones, the and by the external contribution.

Cornering forces can be expressed as the product of the cornering stiffness by the sideslip angle:

$$F_{yi} = -C_i\,\alpha_i = -C_i\left(\beta + \frac{x_i}{V}r - \delta_i\right)$$

The cornering stiffness is always referred to each axle and not of the single wheel. In this way, no allowance is taken for the transversal load transfer and for the camber force owing to the assumption of stiff frame as no roll is considered.

In conclusion, the total lateral linear equations written using the derivative of stabilities are:

$$F_y = Y_\beta \beta + Y_r r + Y_\delta \delta$$

Where:

$$\begin{cases} Y_\beta = -C_1 - C_2 + \frac{1}{2}\rho V^2 S\left(C_y\right)_\beta \\ Y_r = \frac{1}{V}(-aC_1 + bC_2) \\ Y_\delta = C_1 + F_{x1p} \end{cases}$$

The term F_{x1p}, indicating the traction force on the front axle, can be neglected.

Acting similarly to what is done for the lateral direction, the yawning moments are calculated by means of the linearization:

$$M_z = N_\beta \beta + N_r r + N_\delta \delta$$

Where:

$$\begin{cases} N_\beta = -aC_1 + bC_2 + (M_{z1})_\alpha + (M_{z2})_\alpha + \frac{1}{2}\rho V^2 S\, l (C_{Mz})_\beta \\ N_r = \frac{1}{V}(-a^2 C_1 - b^2 C_2 + a(M_{z1})_\alpha - b(M_{z2})_\alpha) \\ N_\delta = aC_1 - (M_{z1})_\alpha \end{cases}$$

2.1.5 Final expression of the equations of motion

On the base of the equations above cited, the final expression of the linearized equations of motion for the handling model is thus:

$$\begin{cases} mV(\dot{\beta} + r) + mV\beta = Y_\beta \beta + \dot{Y_r} r + Y_\delta \delta + F_{ye} \\ J_z \dot{r} = N_\beta \beta + N_r r + N_\delta \delta + M_{ze} \end{cases}$$

These are two first order differential equations for the two unknown β and r. The terms F_{ze} and M_{ze} indicate the generalized external forces applied in y direction and about axis z that cannot be expressed as a function of the two variables [21].

3. Driver model

A road vehicle on pneumatic tires cannot maintain a given trajectory under the effect of external perturbations unless it is controlled by some devices, as it happens in autonomous cars, or more conventionally by a human driver. The driver can be thought as a controller receiving a number of inputs from the vehicle and the environment and outputting a few control signals to the vehicle. With manual control, the driver executes the tasks of the sensors, the controller and the actuators; by adjusting also the power source, even if the control action due to the driver can be assisted by devices as power steering or braking as it occurs in modern cars.

The availability of mathematical models for the driver-vehicle interaction has enormous advantages in the simulation environment; the problem is the effort to translate into mathematical functions concepts so subjective and complicated as the drivability. The difficulties encountered in such a task are so large that many different approaches have been attempted and up to now, there is no standard driver model which can be used in general [22] [23] [24]. They span from very simple linear models to multivariable, nonlinear, adaptive models or models based on fuzzy logic and/or neural networks.

For this job purpose, a simple linearized driver model has been assumed.

There will be explained two simplified models used as reference since they physically represent the limits of the drowsy drivers.

The first one is the not predictive driver model that shows the same behaviour of a drowsy driver at “maximum level”; the second one is the predictive driver that behaves as an alert driver of level 0.

3.1 Not predictive driver model

In building a simple driver model a small number of inputs that the driver receives is selected and very simple control algorithms are chosen to link them with the outputs. The latter are usually the steering angle δ and the position of the pedals respectively of accelerator and brake. In this project, only the first one is considered since the driver model is used in connection with a constant speed handling model. For what is concerned with the inputs instead, the desired trajectory is employed [25].

The controller is assumed to be a tracking system affected by a delay, which is usually assumed as the sum of three distinct physical contributions according to the real human driver behaviour. A reaction time delay, due to the time needed to elaborate the information in the brain, a neuromuscular delay due to the time needed for the command to reach the relevant muscles, and an execution delay due to the time needed to perform and conclude the action.

A simple open-loop transfer function for the linearized driver, in the Laplace domain, is given by:

$$\frac{y(s)}{u(s)} = K_p e^{-\tau s}$$

Where, on the left, the numerator is the output, the denominator the input and on the right there is the transfer function.

By expressing the exponential as a power series reducing it at the first order:

$$\frac{y(s)}{u(s)} \approx K_p \frac{1}{1 + \tau s + \frac{1}{2}\tau^2 s^2} \approx K_p \frac{1}{1 + \tau s}$$

Where K_p is the driver gain, τ the driver delay and s the Laplace variable.

In this case, all the delays previously mentioned are summarized as a single delay τ. Then, trying to replicate a human performance, the input and output of the system have to be chosen. In the simplest case of a linear tracking system, the yaw angle ψ of the vehicle is supposed to be the input and the steering wheel angle

the output. As it happens in normal driving conditions, according to the input, so the trajectory that the driver wants to follow, the output is the steering angle necessary to perform the desired path. Note that the steering ratio must be included if a driver steering has to be monitored, as δ is the angle of the wheels about the kingpin axis and not the one exerted on the steering wheel.

Thus, the transfer function becomes:

$$\frac{\delta(s)}{\psi(s)} = K_p e^{-\tau s} \approx K_p \frac{1}{1+\tau s}$$

That in time domain becomes:

$$\tau\, \dot{\delta}(t) + \delta(t) = -K_p[\psi(t) - \psi_0(t)]$$

Where ψ_0 is the required yaw angle.

Adding this driver representation with the formulas shown in chapter 2 referred to the vehicle dynamics expressed by the derivatives of stabilities, in which the stability depends only on the sideslip angle β and the yaw velocity r so conceptually, they are the outputs; a simple state-space system for linear time-invariant system, can be written:

$$\begin{cases} \dot{z}(t) = A\, z(t) + B\, u(t) \\ y(t) = C\, z(t) + D\, u(t) \end{cases}$$

Where, the terms referred to this project are:

$$z_{np} = \begin{Bmatrix} \beta \\ r \\ \delta \\ \psi \end{Bmatrix}; \quad u_{np} = \{\psi_0\}; \quad y_{np} = \begin{Bmatrix} \beta \\ r \end{Bmatrix}$$

$$A_{np} = \begin{bmatrix} \frac{Y_\beta}{mV} & \frac{Y_r}{mV} - 1 & \frac{Y_\delta}{mV} & 0 \\ \frac{N_\beta}{J_z} & \frac{N_r}{J_z} & \frac{N_\delta}{J_z} & 0 \\ 0 & 0 & -\frac{1}{\tau} & -\frac{K_p}{\tau} \\ 0 & 1 & 0 & 0 \end{bmatrix}; \quad B_{np} = \begin{bmatrix} 0 \\ 0 \\ \frac{K_p}{\tau} \\ 0 \end{bmatrix}$$

$$C_{np} = \begin{bmatrix} 1 & 0 & 0 & 0 \\ 0 & 1 & 0 & 0 \end{bmatrix}; \quad D_{np} = \begin{bmatrix} 0 \\ 0 \end{bmatrix}$$

Where np stands for not predictive so related to the model evaluated up to now contemplating both the dynamic impact and the driver without any projecting influence. The more interesting equation is the dynamic one that written in its entire form is:

$$\begin{Bmatrix} \dot{\beta} \\ \dot{r} \\ \dot{\delta} \\ \dot{\psi} \end{Bmatrix} = \begin{bmatrix} \frac{Y_\beta}{mV} & \frac{Y_r}{mV} - 1 & \frac{Y_\delta}{mV} & 0 \\ \frac{N_\beta}{J_z} & \frac{N_r}{J_z} & \frac{N_\delta}{J_z} & 0 \\ 0 & 0 & -\frac{1}{\tau} & -\frac{K_p}{\tau} \\ 0 & 1 & 0 & 0 \end{bmatrix} \begin{Bmatrix} \beta \\ r \\ \delta \\ \psi \end{Bmatrix} + \begin{bmatrix} 0 \\ 0 \\ \frac{K_p}{\tau} \\ 0 \end{bmatrix} \{\psi_0\}$$

Combining the static part, referred to the output, a total depiction of the model is achieved:

$$\begin{Bmatrix} \beta \\ r \end{Bmatrix} = \begin{bmatrix} 1 & 0 & 0 & 0 \\ 0 & 1 & 0 & 0 \end{bmatrix} \begin{Bmatrix} \beta \\ r \\ \delta \\ \psi \end{Bmatrix} + \begin{bmatrix} 0 \\ 0 \end{bmatrix} \{\psi_0\}$$

By these two last equations, stated through the state space, the not predictive driver model is designed.

This simple model is nevertheless too simple to yield useful results. The lack of predictive behaviour and the unrealistic assumption that the driver reacts only to the yaw angle makes such a driver quite unstable. Having no prediction, the system always acts late, getting as input the reference point that the vehicle should have at the same time it receives the instantaneous position. Moreover, the absence of feedback makes the system unable to be controlled in real-time.

3.2 Predictive driver model

It is a common experience that, when a driver takes as reference a point very close to the front of the vehicle, like when driving in the fog, an oscillatory trajectory is usually obtained while the oscillations disappear if the reference point is far ahead so adding a real involvement due to the scenario ahead of the car user.

A simple way to incorporate a sort of projecting behaviour into the model is that of using as error not only the difference between the desired and the actual value of the yaw angle, but also the lateral distance between a point on the longitudinal direction stated by the x axis, located at a given distance L in front of the vehicle and the required trajectory (distance d).

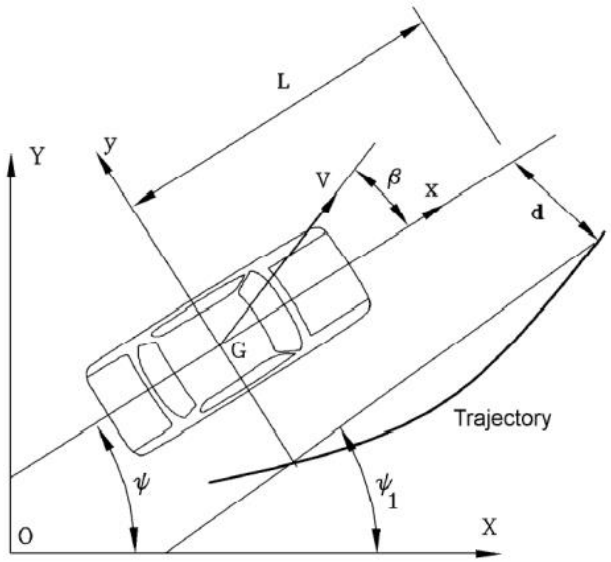

Figure 11: Predictivity concept

With simple computations and assuming that the angular error $\psi - \psi_1$ is small the lateral distance error d can be approximated as:

$$d = L\,(\psi - \psi_1 + \frac{y}{L})$$

Where y according to the body-fixed reference frame is the lateral displacement computed as integral of the lateral component v of the total speed V. Since the speed of the vehicle is constant, with the previous linearization in the second chapter:

$$\dot{y} = V\beta$$

The angle $\psi_1$instead, can be easily computed from the shape of the trajectory as the angle between X-axis and a line passing through two points of the trajectory at a distance L.

At the end, the equation expressing the time domain model of the driver, adding the anticipation to the not predictive model turn out to be:

$$\tau\,\dot{\delta}(t) + \delta(t) = -K_p\left[\psi(t) - \psi_1(t) + \frac{y(t)}{L}\right]$$

Introducing into the mathematical open-loop model of the linearized vehicle and operating in the same way as for the previous model, the new state equations of the vehicle-driver system are expressed by:

$$z_p = \begin{Bmatrix}\beta\\ r\\ \delta\\ \psi\\ y\end{Bmatrix}; \quad u_p = \{\psi_1\}; \quad y_p = \begin{Bmatrix}\beta\\ r\end{Bmatrix}$$

$$A_p = \begin{bmatrix} \frac{Y_\beta}{mV} & \frac{Y_r}{mV} - 1 & \frac{Y_\delta}{mV} & 0 & 0\\ \frac{N_\beta}{J_z} & \frac{N_r}{J_z} & \frac{N_\delta}{J_z} & 0 & 0\\ 0 & 0 & -\frac{1}{\tau} & -\frac{K_p}{\tau} & -\frac{K_p}{L\tau}\\ 0 & 1 & 0 & 0 & 0\\ 0 & V & 0 & 0 & 0 \end{bmatrix}; \quad B_p = \begin{bmatrix}0\\0\\ \frac{K_p}{\tau}\\0\\0\end{bmatrix}$$

$$C_p = \begin{bmatrix}1 & 0 & 0 & 0 & 0\\ 0 & 1 & 0 & 0 & 0\end{bmatrix}; \quad D_p = \begin{bmatrix}0\\0\end{bmatrix}$$

Where p stands for predictive driver.

Putting the dynamic and input gain matrix together:

$$\begin{Bmatrix} \dot{\beta} \\ \dot{r} \\ \dot{\delta} \\ \dot{\psi} \\ \dot{y} \end{Bmatrix} = \begin{bmatrix} \frac{Y_\beta}{mV} & \frac{Y_r}{mV} - 1 & \frac{Y_\delta}{mV} & 0 & 0 \\ \frac{N_\beta}{J_z} & \frac{N_r}{J_z} & \frac{N_\delta}{J_z} & 0 & 0 \\ 0 & 0 & -\frac{1}{\tau} & -\frac{K_p}{\tau} & -\frac{K_p}{L\tau} \\ 0 & 1 & 0 & 0 & 0 \\ 0 & V & 0 & 0 & 0 \end{bmatrix} \begin{Bmatrix} \beta \\ r \\ \delta \\ \psi \\ y \end{Bmatrix} + \begin{bmatrix} 0 \\ 0 \\ \frac{K_p}{\tau} \\ 0 \\ 0 \end{bmatrix} \{\psi_1\}$$

And the static contribution:

$$\begin{Bmatrix} \beta \\ r \end{Bmatrix} = \begin{bmatrix} 1 & 0 & 0 & 0 & 0 \\ 0 & 1 & 0 & 0 & 0 \end{bmatrix} \begin{Bmatrix} \beta \\ r \\ \delta \\ \psi \\ y \end{Bmatrix} + \begin{bmatrix} 0 \\ 0 \end{bmatrix} \{\psi_1\}$$

Both the analysed driver models are a severe oversimplification of the actual human behaviour, but the last one already operates in an acceptable way many requests and in fact, it has been implemented in the design of the drowsy driver. As already stated, more complex and realistic models can be found in the literature [22] [23] [24].

3.3 Adopted driver model

In this section, a short explanation of the theoretical model used in the modelling of the driver is presented. Using as reference the predictive model explored above, only the variations are shown.

The main difference from the models seen in the literature is referred to the driver action. It is not just characterized by a proportional gain therefore proportional to the error, but also by an integrative gain. This term accounts for past values of the error and integrates them over time. If there is a residual error after the application of proportional gain, the integral term seeks to eliminate it by adding

a control effect due to the historic cumulative value of the inaccuracies. When the error is eliminated, the integral term will cease to grow.

Hence, all the previous equations change.

The transfer function is converted to:

$$\frac{\delta(s)}{\psi(s)} = (K_p + \frac{K_i}{s})e^{-\tau s} \approx (K_p + \frac{K_i}{s})\frac{1}{1+\tau s}$$

That in time domain becomes:

$$\tau\,\dot{\delta}(t) + \delta(t) = -K_p\left[\psi(t) - \psi_1(t) + \frac{y(t)}{L}\right] - K_i\int\left[\psi(t) - \psi_1(t) + \frac{y(t)}{L}\right]dt$$

The state-space equations are not taken into account in this division since as it will be explained in the next chapter, this way of description is not the best one in terms of adjustments and inspection of the features.

4. Practical implementation

In this fourth chapter, the practical application of the theory is presented in the MathWorks environment: Matlab and Simulink.

First of all, the not predictive and predictive model will be examined, then the "drowsy model" is explained based on the previous two.

4.1 Driver model execution

According to chapter 3, the not predictive open loop system and the predictive closed loop system can be approximated in matrix formulation with a state space procedure. For what is concerned the model adopted in the level subdivisions of the drowsy driver a different approach will be used.

4.1.1 Not predictive model

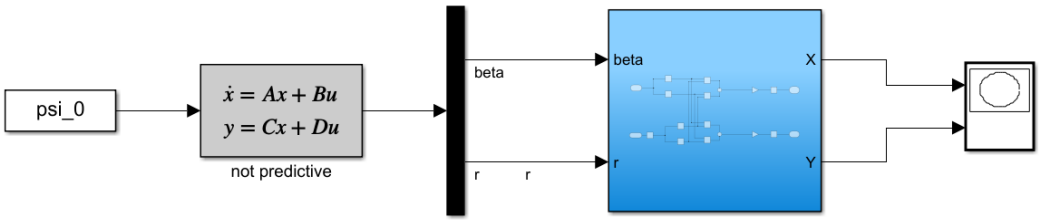

Figure 12: Not predictive model

As it is possible to notice in the picture above, the modelling is really simple.

The system is represented by an open loop structure deprived of a feedback connection able to instantaneously correct the trajectory in real time. It does not use feedback to determine if its output has achieved the desired goal.

In this case, the driver corresponds to the controller and the plant is equal to the vehicle. In the open loop control, the input does not depend on the output because the controller is not aware of what is actually happening to the variables having no feedback link and thus it does not allow the stabilization of unstable systems [26].

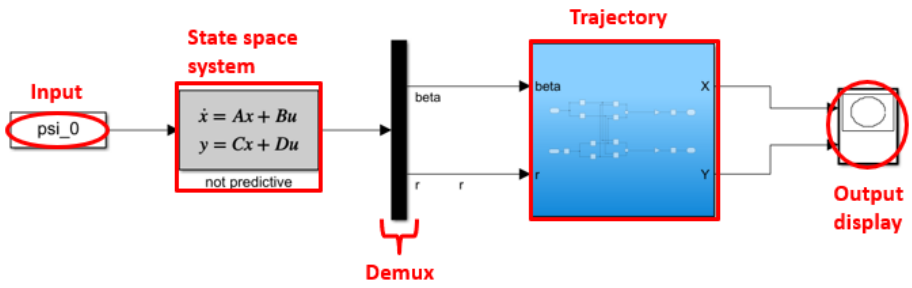

Figure 13: Open loop blocks

More in detail, as depicted in the scheme, the not predictive system is modelled with five blocks. Ordered from the left: the input, given in angular terms of yaw using a time-series format in order to have at each time instant the desired goal; the state space block in which there are all the equations, described in chapter 2, in the matrices $A_{np}, B_{np}, C_{np}, D_{np}$; the demux that extracts the components of the input vector, so the output y_{np} and it separates the signals in order to generate the conducted trajectory starting from β and r.

Knowing that:

$$\begin{cases} X(t) = \int_0^t [V cos(\psi) - V\beta \sin(\psi)]du \\ Y(t) = \int_0^t [V sin(\psi) - V\beta \cos(\psi)]du \end{cases}$$

And it is computed in the blue block:

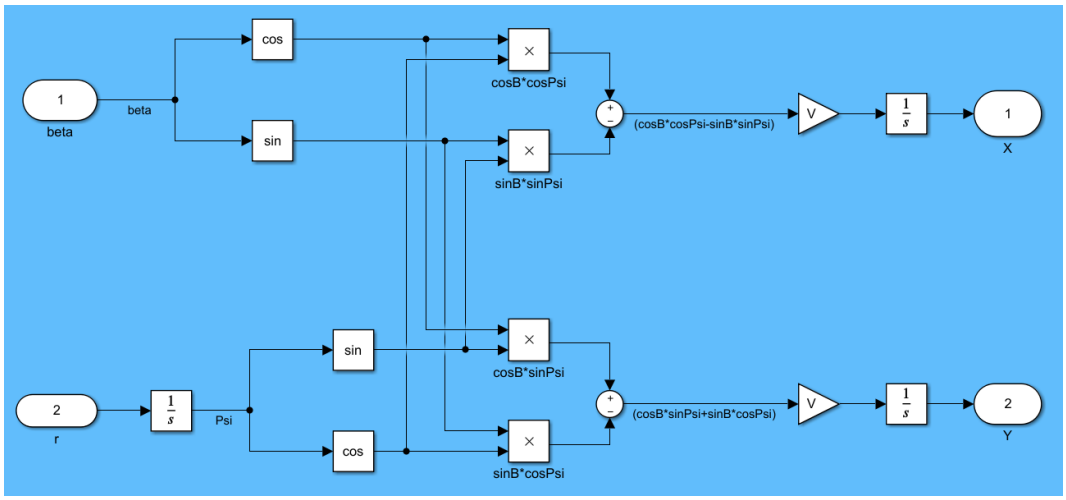

Figure 14: Trajectory computation

In the picture above, B stand for β.

The last block is the display used to show the carried out path in the inertial reference frame X- Y.

4.1.2 Predictive model

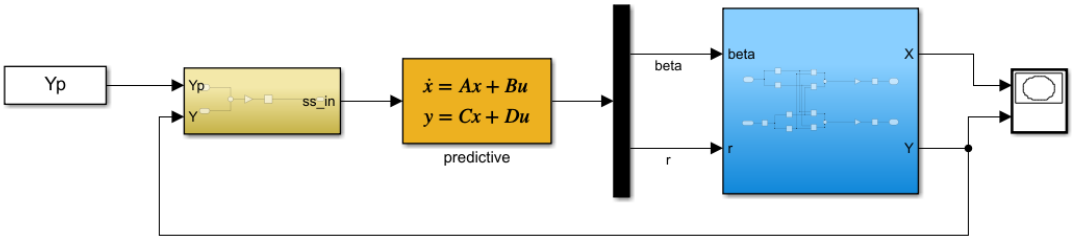

Figure 15: Predictive model

Again, the simplicity of the model is evident. In this case although, the feedback link is present and it is the most important difference with respect to the not predictive system, providing, in this case, a closed loop controller. In closed loop control, the command action from the controller is dependent on the process output. Therefore, it has the feedback connection which ensures the controller

exert a control action to give a process output the same as the "reference input" correcting at each time t the system behaviour.

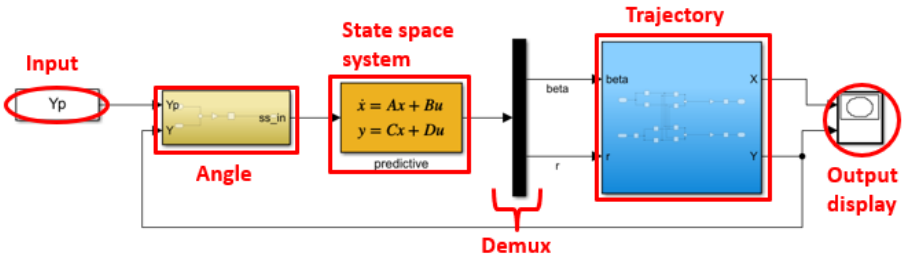

Figure 16: Closed loop blocks

Also for this case, a brief explanation of the blocks is provided. The total model is made of 6 blocks. The input, this time given as a distance measurement and not in angle, is the ideal trajectory expressed in the global lateral coordinate Y. It is used as reference since the angle is computed as difference with the actual position in the next block. This offers a larger versatility because it is easier to impose the trajectory in a space variable with respect to the other not predictive case in which it is necessary to have the trajectory created in angles. It's important to notice that the values utilized as reference, again supplied in time-series format, are already taking into account the predictivity. The detailed clarification of this concept will be examined in the next chapter.

The yellow block is used to calculate the angles that the state space system needs in order to get the variables β and r as is displayed below:

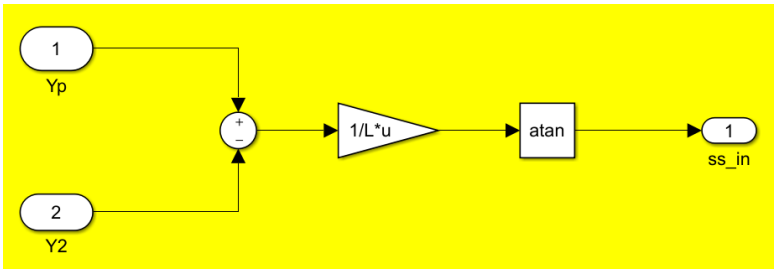

Figure 17: Angle computation

The yaw angle is calculated using a trigonometric function and keeping in mind the predictivity. The remaining is the same as in the configuration of the not predictive driver, there are the demux, the trajectory computation block in blue and the display to evidence the path in the global reference frame X- Y.

4.2 Drowsy driver model construction

The previous models are really simple and easy to use but they don't allow the possibility to monitor the variables inside the state space, unless the outputs and they don't permit any changing in the system according to some physical and real limits. For these reasons, block modelling is employed in order to design the different drowsy drivers, enabling variations and corrections.

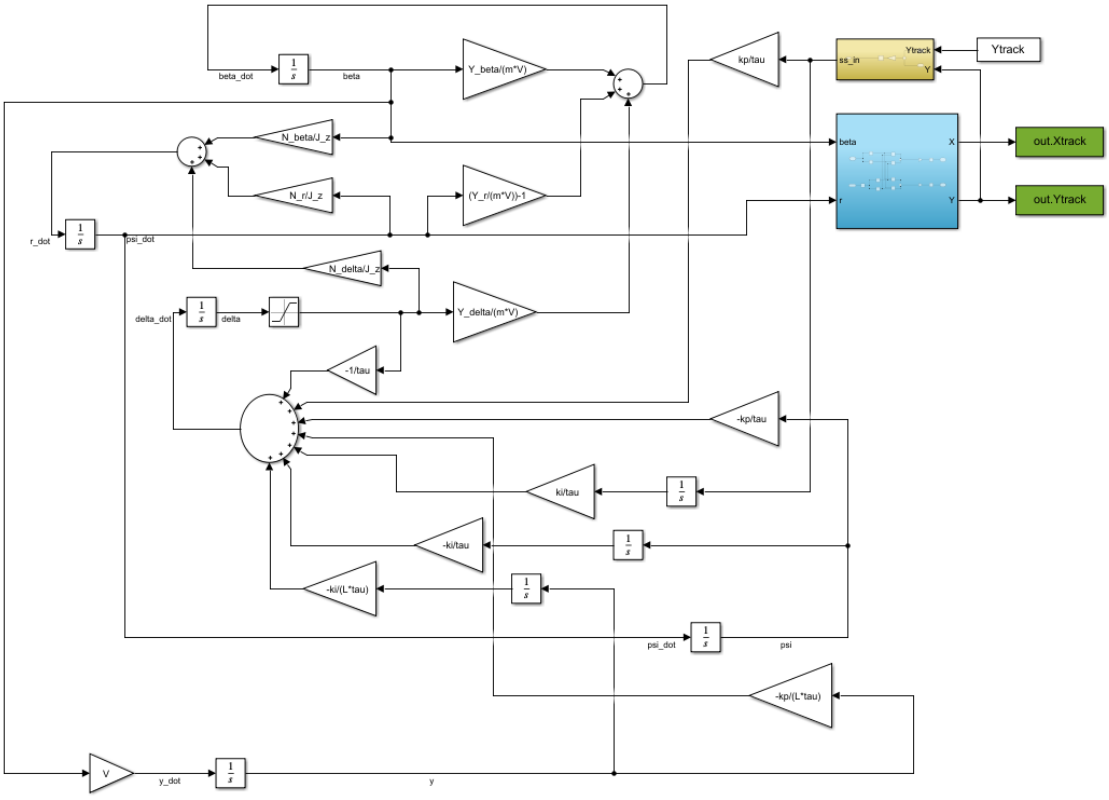

Figure 18: Drowsy driver model

As already stated in section 3.3, the drowsy driver model, for what is concerned the theory behind the system, is based on the predictive model with the addition of the integral contribute.

All the links derive from the differential equations that govern the dynamic:

$$\begin{cases} \dot{\beta}(t) = \frac{Y_\beta}{mV}\beta(t) + \left(\frac{Y_r}{mV} - 1\right) r(t) + \frac{Y_\delta}{mV}\delta(t) \\ \dot{r}(t) = \frac{N_\beta}{J_z}\beta(t) + \frac{N_r}{J_z} r(t) + \frac{N_\delta}{J_z}\delta(t) \\ \dot{\psi}(t) = r(t) \\ \dot{y}(t) = V\beta(t) \\ \dot{\delta}(t) = -\frac{\delta}{\tau} - \frac{K_p}{\tau}\left[\psi(t) - \psi_1(t) + \frac{y(t)}{L}\right] - \frac{K_i}{\tau}\int\left[\psi(t) - \psi_1(t) + \frac{y(t)}{L}\right] dt \end{cases}$$

The firsts four equations are referred to the vehicle dynamics and the last one to the driver model. These are five differential equations effortlessly implemented on Simulink that represent the new system. The input and the output are equal to the predictive configuration, so with the angular computation starting with the feedback values in the yellow block and the red block for the route taken.

A small zoom in the driver equation represented in Simulink has to be done with the purpose of highlighting an important physical limitation:

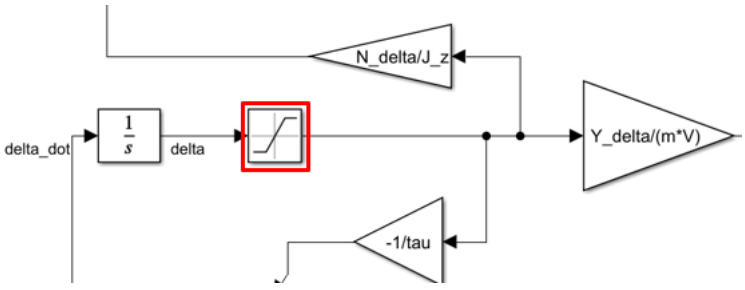

Figure 19: Saturation block

In red the saturation symbol applied to the steering angle δ is evidenced. Realizing different drowsy driver levels from alert conditions to more critical ones, unstable circumstances can occur. In this case, a physical limitation is due to the wheel arch

compartment and steering system. The wheel is not able to rotate more than 30-35 degrees with respect to its kingpin axis, so it is necessary to put a saturation in order to keep the maximum possible value without having further risen. The limits expressed in radiant degrees are 0.5 and -0.5. Doing this, also the more critical condition takes into account the overall dimensions and the reality of the representation is preserved.

4.3 Pseudocode

Coupled with the Simulink environment, a matlab code has been prepared in order to initialize the variables, provide the inputs to the model and graphically analyse the results having greater customization. The procedure is the same for both the manoeuvre used in this project: the double lane change and the open track; uncommenting the desired parts. The adopted numerical values are referred to a generic compact SUV. Below, all the steps followed to achieve the outcomes are shown in a pseudocode layout; consequently comments are present to have a better understanding of the language.

```
DATA       % upload geometrical data from .m file

V=80/3.6;  % cruise speed in m/s

%% Derivatives of stability and relative formula

Y_beta; Y_r ; Y_delta; N_beta; N_r ; N_delta;

%% Definition of the trajectory

B=1.8; % width of the vehicle in m

Y=zeros(1,125);       % vector initialization equal to zero
psi_0=zeros(1,125);   % vector initialization equal to zero

% double lane manouvre

    for X=1:125

        if X<15
          Y(X)=0;
          psi_0(X)=0;
```

```
   elseif 15<=X && X<45
          Y(X)=3.5/2*(1-cos(pi/30*(X-15)));
          psi_0(X)=atan(3.5*pi/60*sin(pi/30*(X-15)));


   elseif 45<=X && X<70
          Y(X)=3.5;
          psi_0(X)=0;


   elseif 70<=X && X<95
          Y(X)=3.5/2*(1+cos(pi/25*(X-70)));
          psi_0(X)=-atan(3.5*pi/50*sin(pi/25*(X-70)));


       else X>=95
          Y(X)=0;
          psi_0(X)=0;

       end
    end

X=1:125;

% travelled distance

road_double=15+sqrt(30^2+3.5^2)+25+sqrt(25^2+3.5^2)+30;

% Other road segments classification

% 1st bend 45° left

th1 = linspace(3*pi/2,7*pi/4);
Rlat1 = 30;                     % lateral radius
Rlong1= 40;
C1 = [max(X) Rlat1] ;           % curve centre
x1 = C1(1)+Rlong1*cos(th1);     % longitudinal distance
y1 = C1(2)+Rlat1*sin(th1);      % lateral distance

semicircle1=pi*(Rlat1+Rlong1)/2;
road1=semicircle1/4;            % travelled distance

% 1st straight

straight1= 20;   % in [m]
Xstraight1=linspace(max(x1),max(x1)+straight1);
Ystraight1=linspace(max(y1),max(y1)+straight1);

% travelled distance
road_rectilinear1=sqrt(2*(straight1^2));
```

```
%% all the other segments

% 2nd bend pi/2

% 2nd straight

% 3rd bend 45° left

% 3rd straight

%% total travelled distance

distance=road_double  % considering only the double lane

distance=road_double+road1+road_rectilinear1+road2+road_rect
ilinear2+road3+straight3;

%% Xtrack & Ytrack definition
% they indicate the total longitudinal and lateral coordinates
% expressed in the inertial reference frame

Xtrack=[X];     % considering only the double lane
Ytrack=[Y];     % considering only the double lane

Xtrack=[X x1 Xstraight1 x2 Xstraight2 x3 Xstraight3];
Ytrack=[Y y1 Ystraight1 y2 Ystraight2 y3 Ystraight3];

% time subdivision for each street

timedouble=linspace(0,road_double/V,125);

time1bend=linspace(timedouble(end),timedouble(end)+road1/V);
timestraight1=linspace(time1bend(end),time1bend(end)+road_re
ctilinear1/V);
time2bend=linspace(timestraight1(end),timestraight1(end)+roa
d2/V);

% … same for all the remaining road segments

%% total driving time

timevals=[timedouble]      % considering only the double lane

timevals=[timedouble   time1bend   timestraight1   time2bend
timestraight2 time3bend timestraight3];

% ideal coordinates vs time in both the directions

t_Ytrackideal=timeseries(Ytrack,timevals);
t_Xtrackideal=timeseries(Xtrack,timevals);
```

```
%% LEVEL 0
% level identification

kp0=0.6;
ki0=0.12;
tau0=0.05;    %[s]
L0=10;        %[m]

timevals0=timevals-L0/V;         % predictive effect

% input parameter in the model for level 0

t_Ytrack0p=timeseries(Ytrack,timevals0);

% … same for all the levels up to 4

%% TRAJECTORY PLOTS vs X

figure

sim open_track_drowsy      % simulation file .slx with model

c=flip(hot(8));            % colour customization

hold on

axis equal

xlim([min(Xtrack)-10 max(Xtrack)+10]);
ylim([min(Ytrack)-5 max(Ytrack)+5]);

xlabel('X [m]')
ylabel('Y [m]')

title('Drowsiness levels in the track')

% plots using Simulink output

% ideal; LEV 0-1-2-3-4

legend  ({'Ideal  trajectory','Level  0','Level  1','Level
2','Level 3','Level 4'},'AutoUpdate','off');

%% right track lanes vs X

road_width=3.5;       % in [m]

% lanes of the second curve

Yleftlane=ans.Yideal+road_width/2;
Yrightlane=ans.Yideal-road_width/2;

% plot of the road
```

```
hold off

%% TRAJECTORY PLOTS vs t

% … same as vs X changing the first variable with time
```

5. Scenario

Having explained how the system has been designed using Matlab and Simulink, before showing the results, the scenario used as reference for the drowsy driver discretization and the open track created to verify the behaviour in a different environment with respect to the one in the testing is presented.

5.1 Manoeuvres

In this project two different manoeuvres have been employed: the first one, the double lane change is used as reference in the development phase of the different drowsiness levels; whereas the second one is exploited in order to verify the effectiveness of the parametrisation in an open trail.

5.1.1 Double lane change

The double lane change manoeuvre is a standardized trajectory used to test vehicle stability. It simulates overtaking starting from the right road, so there is a first bend to the left to merge onto the fast lane and after a straight, a right bend is essential to come back in the previous street.
A first image is presented in an easy to read scale in order to display the differences between the lanes and the ideal trajectory. It will be also adopted during the analysis of the results with the intention of zoom between the different levels.

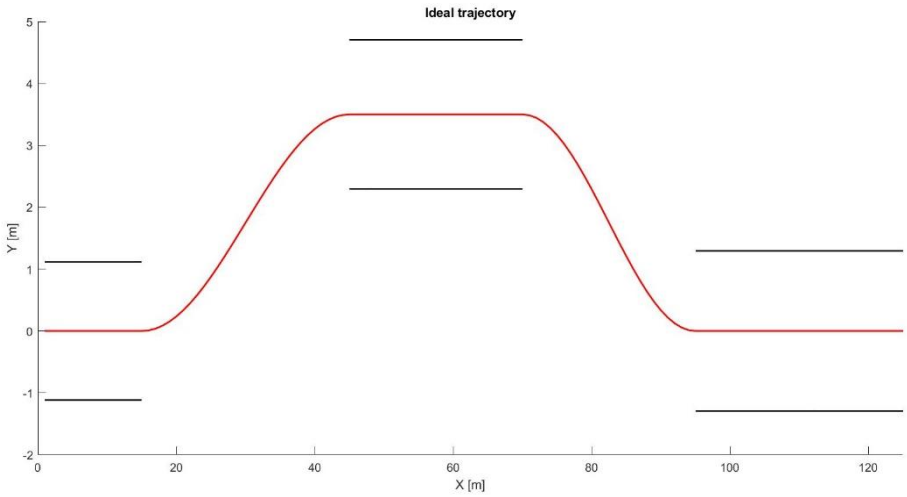

Figure 20: Double lane change

More accurately it requires that the vehicle travels for 15 meters in the original lane, to change lane with a lateral displacement of 3.5 meters in 30 meters, to stay in this lane for 25 meters and to return to the original lane in the other 25 meters. The width of these lanes depends on the width of the vehicle used in the test and every straight segment has an increment in the thickness delimitated by cones. In meters, denoting B as width of the vehicle, is 1.1 B + 0.25 for the first lane, 1.2 B + 0.25 for the second and 1.3 B + 0.25 for the third. It's important to notice that also the largest road is smaller than the real highway lane.

The analytical function that describes the ISO double lane change is function of the longitudinal distance defined in lateral and angular terms [21]:

$$
\begin{aligned}
&for\ X < 15 && Y = 0 \\
&for\ 15 \leq X < 45 && Y = \frac{3.5}{2}\left\{1 - cos\left[\frac{\pi}{30}(X - 15)\right]\right\} \\
&for\ 45 \leq X < 70 && Y = 3.5 \\
&for\ 70 \leq X < 95 && Y = \frac{3.5}{2}\left\{1 + cos\left[\frac{\pi}{25}(X - 70)\right]\right\} \\
&for\ 95 \leq X < 125 && Y = 0
\end{aligned}
$$

$$for\ X < 15 \qquad \psi_0 = 0$$

$$for\ 15 \leq X < 45 \qquad \psi_0 = arctan\left\{\frac{3.5\pi}{60} sin\left[\frac{\pi}{30}(X - 15)\right]\right\}$$

$$for\ 45 \leq X < 70 \qquad \psi_0 = 0$$

$$for\ 70 \leq X < 95 \qquad \psi_0 = -arctan\left\{\frac{3.5\pi}{50} sin\left[\frac{\pi}{25}(X - 70)\right]\right\}$$

$$for\ 95 \leq X < 125 \qquad \psi_0 = 0$$

In which, clearly the straight sections are characterized by a constant Y and null ψ_0 since the vehicle has the same orientation compared to the inertial position, while in the transient, both the parameters are approximated by a trigonometric function and are obviously not constant.

Considering a scaled plot the result is this:

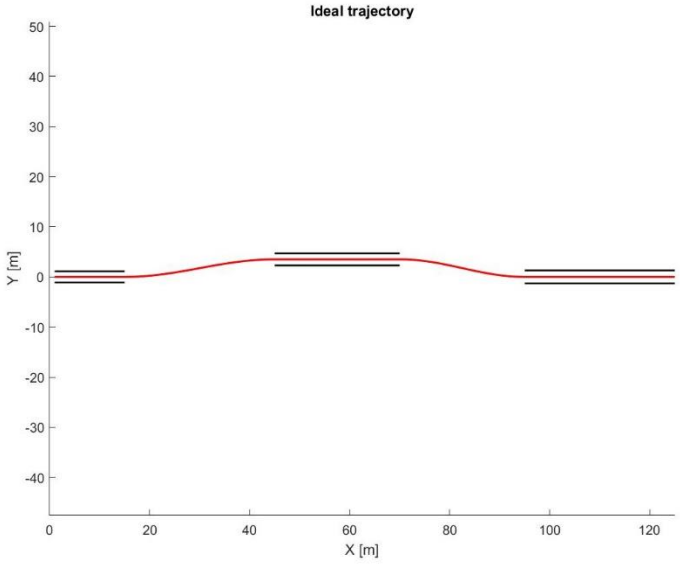

Figure 21: Real view of the double lane change

Scaling the axles, the real view of the road is shown giving a better understanding of the physical situation. Also because the manoeuvre must be performed at a constant speed equal to 80 km/h and without giving the right top view the manoeuvre seems impossible to follow. The same speed is considered also for the open track.

The lane changes must be performed providing that none of the cones delimiting the three straight lanes are touched in order to accomplish a positive result, otherwise, the test is failed.

5.1.2 Open track

The second path is made of different road segments added to the previous double lane change manoeuvre reaching a total of seven roads.

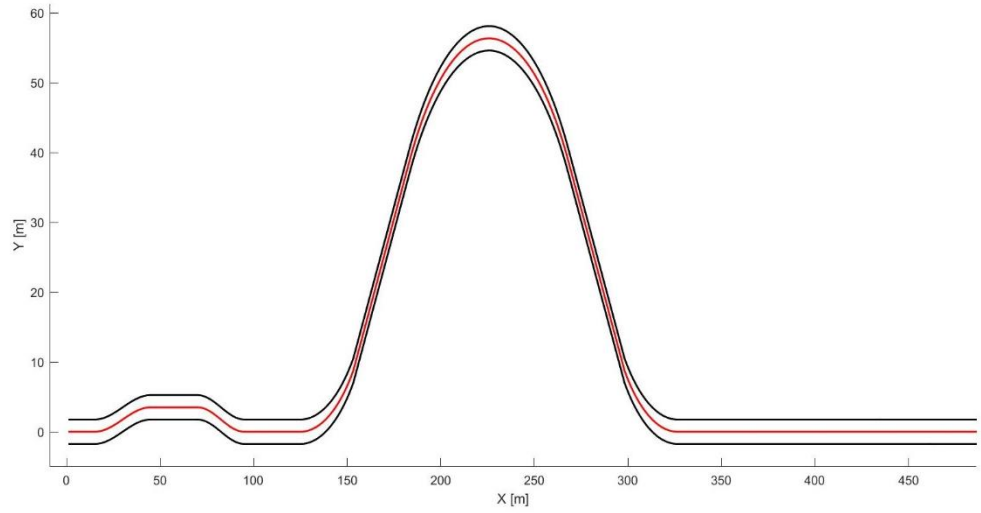

Figure 22: Open track

As before, this representation does not take into account the real dimension of the road but it is reported since it is easier to see the centreline and in general all the different levels of tiredness.

Considering the speed at which the test is performed and the type of vehicle, the route has been designed in this way:

- 1st curve to the left of 45° with a longitudinal radius of 40 meters and a lateral one of 30;
- A linear road of 30 meters;
- 2nd bend to the right of 90° with a radius of 60 meters;

- Another straight road of 30 meters;
- 3rd curve to the left of 45° with a longitudinal radius of 40 meters and a lateral one of 30;
- Final straight of 150 meters.

On the right, there is the real view from the top.

In order to see the path in this vertical view, a rotation of the reference system has been done. In this way, on the horizontal axis, the lateral position is shown in which negative values mean moving towards the left and vice versa for curve to the right. On the vertical axis instead, the simple longitudinal travelled distance is highlighted.

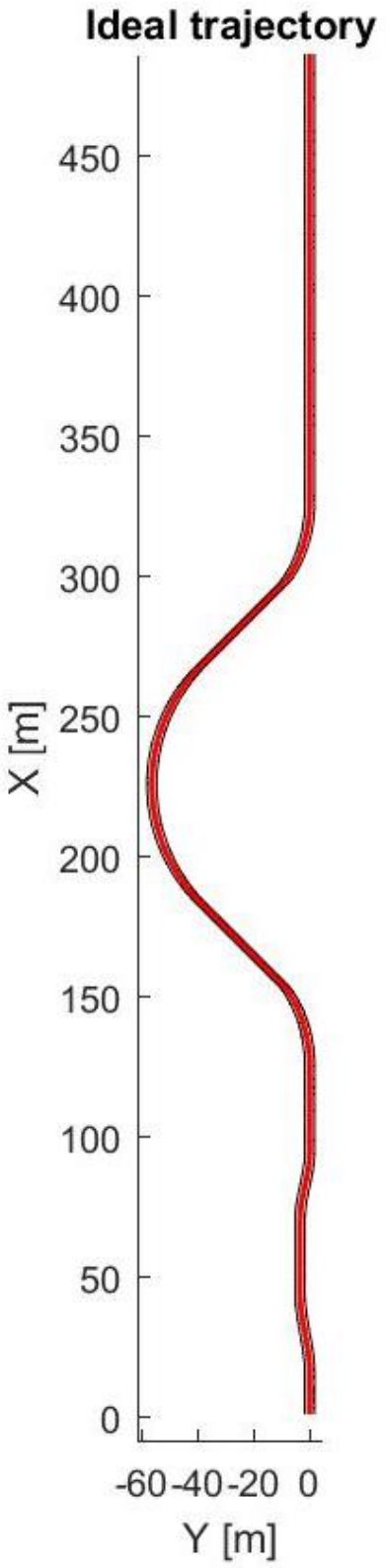

Figure 23: Real view of the open track

6. Discretization of the sleepiness levels

In this chapter, the drowsiness levels are described, in terms of variable used in the setting for the discretization of the different drivers. First of all the tuning of the PI coefficients will be examined in order to set for each fatigue level its parametrisation; then, the other limits dictated by the human contribution, the time delay and the predictivity are added.
According to the last section of chapter 3 related to the drowsy driver model and the driver model in general, the car user is considered as the controller and the vehicle is the plant so the object that needs to be controlled. The assumption was to have a driver effect expressed by a proportional action and an integral one, due to this it is approximated by a PI system.

6.1 PI tuning

The Proportional-Integral-Derivative controller, commonly abbreviated as PID, is a negative feedback system widely used in automatic control and in the industry. The Proportional-Integral variation, PI, is the most popular so the one chosen for this project. Thanks to an input that determines the current value, it is able to react to a possible positive or negative error tending towards the value 0 minimizing the inaccuracy over time. The reaction to the error can be adjusted and this makes this system very versatile. The optimization is performed using two control terms: the proportional and integral influence. Its form in the Laplace domain is:

$$C(s) = K_p + \frac{K_i}{s}$$

Where C means controller and it is the sum of the two contributes: proportional K_p and integral K_i. These terms work together in parallel, in the same position of the chain depicted below:

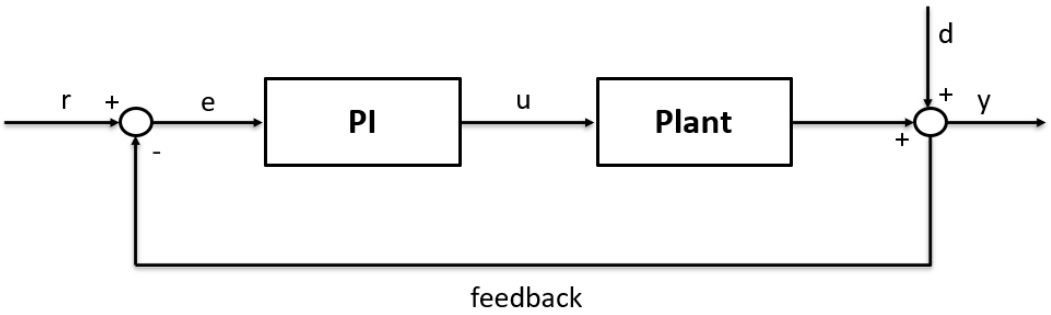

Figure 24: PI system

Where in the PI block there are K_p and K_i in parallel; r is the reference also called the desired setpoint SP; $e(t)$ is the error, function of the time, equal to the difference between the required values and the output line taken from the feedback link with a negative sign so that, it is obtained: $e(t) = r(t) - y(t)$. The product $y(t)$ is also called process variable PV. The plant in this project is the vehicle as previously enounced, described by the vehicle model explained in the chapter 2. The disturbances d are taken into account considering an external input added to the exit of the plant block [26].

The main features of this controller are the simplicity in the control design techniques and that it allows online tuning on the real system to control.

Looking more in detail into the parameters used in the characterisation of the sleepy driver K_p and K_i:

- K_p is proportional to the current value of the error $SP - PV$. If the error $e(t)$ grows or shrinks, the control output will increase or drop according to the gain factor. Using proportional control alone will result in an error between the reference and the actual process value because it requires an error to generate the proportional response.

  If there is no error, there is no corrective response. The past history and current trajectory of the controller error have no influence on this computation.

- K_i accounts for past values of the $SP - PV$ error and integrates them over time to produce the integrational I term. If there is a residual inaccuracy after the application of proportional control, the integral term seeks to eliminate the residual error by adding a control effect due to the historic cumulative value of the error. Integration is a continual summing of errors over time that is added up from the beginning up to the present time. In practice, how long and how far the measured process variable is from the setpoint over time. When the error is eliminated, the integral term will cease to grow and remains constant [27].

A brief overview of the practical effect induced by these factors is clarified analysing an own step response based on an invented transfer function, so not referred to the vehicle model:

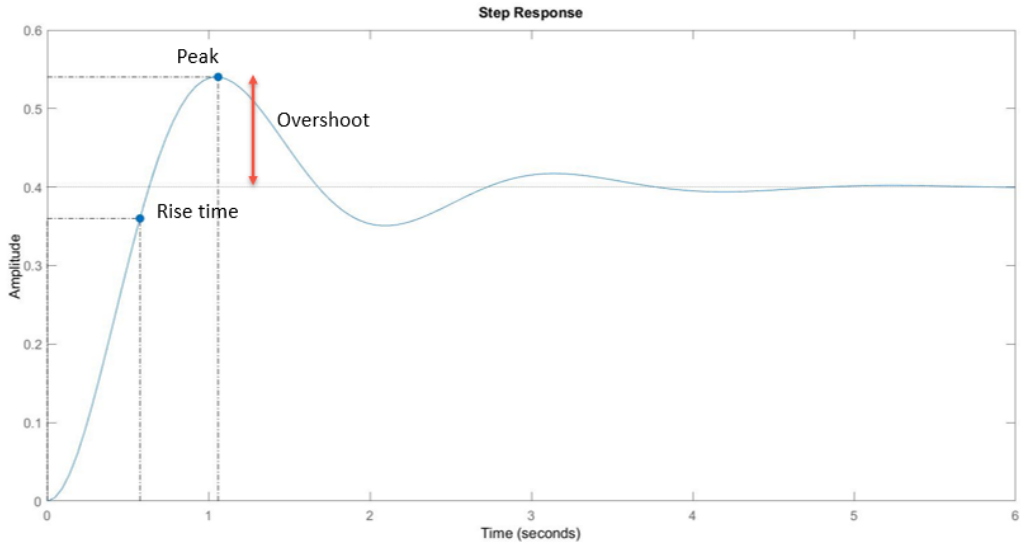

Figure 25: Step response

Where, the rise time is the time required for the signal to increase from one specified value, expressed as a percentage of the steady-state value and the 90% of the same. In this case, it is the time necessary for the system to reach 90% of

the final constant value starting from 0%. More often is the time needed to get 90% from 10%.

The peak is the maximum amount attained during the step response and from it, the overshoot is computed as the difference with respect to the constant stable value; it can be also defined in percentage.

Adopting K_p and K_i, it is important to examine the effect of these parameters in the system to avoid useless attempts and to understand and evaluate the results according to the theoretical expectations [28].

In the table below, the induced effect increasing one variable at a time is shown:

	Rise time	Overshoot	Steady-state error
K_p	*Decrease*	*Increase*	*Decrease*
K_i	*Decrease*	*Increase*	*Eliminate*

Figure 26: Effect of gain variations

Physically, these coefficients are representing the driver effort on the steering wheel; nevertheless neglecting the transmission ratio of the steering system it is an action directly applied to the tire at the ground level. Greater is the car user action, greater will be the gain. Studying the normal driving behaviour it is possible to state that an alert driver corrects the desired trajectory almost all the time with small micro corrections; that mathematically speaking corresponds to small K_p and K_i. Vice versa for a drowsy driver, higher is the tiredness level and lower will be the number of adjustments with abrupt corrections when they occur. In the critical situation, no modifications are exerted by the car user and skidding off the road is unavoidable.

The numerical range is between 0.1 and 2, however a small subsystem of it has been considered in order to design drivers very near to each other avoiding situations too unstable.

6.2 Driver delay and predictivity

Beyond the gain coefficients that describe the action of the driver in terms of strength, its promptness and predictivity have to be added.

The driver is affected by a delay, which is usually assumed as the sum of three distinct physical influences according to the real human performance:

- a reaction time delay, that is the time needed to elaborate the information in the brain and the beginning of the message phase;
- a neuromuscular delay, due to the time required for the command sent from the brain to reach the relevant muscles and;
- an execution delay due to the time needed to perform and conclude the action.

All these effects are collected in a unified delay called simply τ that intrinsically takes into account all the human phases. According to the driver experience and professionality, τ is spanned between 0.05 and 0.25. Generally, a superfast response is attributed to an expert pilot, whereas the larger values are referred to normal users of passenger cars.

In this project, the allocation adopted is not the one accepted in the literature but it has been properly created to reach the desired discretization, so in case of a small delay equal to 0.05 it doesn't mean that a professional driver has been considered to execute the manoeuvre, but only that, the result using that value is coherent and useful in the creation of that particular level.

The last variable considered in the design phase is the predictivity L.

As earlier explained in chapter 3 in the predictive driver model, it represents a rough approximation of how the human body is used to follow its wanted path during travel. Considering the predictivity L, the actions performed by the driver are based on what there is ahead of him. In practice, the input analysed in the Simulink model, at a certain time, is shifted towards the future position and taken as a reference to establish eventual adjustments in the meantime. A low value of L indicates low predictivity, so representative of more tired driver since sudden

recognition of the road occur. This induces a further delay in the system. High values of predictivity, instead are referred to a more alert driver that drives looking far from him. There are also limitations because numbers too high create an unstable system exceeding the real human vision anticipating too many the commands with respect to the current position of the vehicle.
It is important to evidence that the limitations of this model with a fixed predictivity along all the paths are a strong assumption since a real human driver adapts the forecast at any moment.

6.3 Levels

In the end, the discretization of drowsiness levels is accomplished by matching four variables, two derived from the proportional and integral controller and the lasts from the study of human behaviour:

1. K_p as proportional factor;
2. K_i as history factor;
3. τ as driver lag;
4. L as predictivity.

As already repeated, the subdivision in tiredness levels is performed in a narrow road zone, in the proximity of the centreline in order to avoid simulating dangerous situations. The next table is the result of several simulations done to achieve the desired differences between the sleepy drivers. So it comes from an inverse process: following the control theory and the distinctive features of the drowsiness, an attempt is created and then looking at the results in the tracks it is validated or not.
Knowing that the driver delay is expressed in seconds and the predictivity in meters; the best characterization chosen is:

	Level 0	Level 1	Level 2	Level 3	Level 4
K_p	**0.6**	**0.65**	**0.7**	**0.75**	**0.8**
K_i	**0.12**	**0.13**	**0.14**	**0.15**	**0.16**
τ	**0.05**	**0.08**	**0.11**	**0.14**	**0.16**
L	**10**	**9.5**	**8.5**	**8**	**7.5**

Figure 27: Parametrisation of the levels

The colours combined with the numbers are identifying the distinct intensities, especially in the plots, starting with the lighter colour for the vigilant driver to the darker representative of the more drowsy.

According to the theory, increasing the sleepiness level the trend of the variables is compliant, so that:

- K_p increases of 0.05 every step;
- K_i increases of 0.01 every step;
- τ increases of 0.03 seconds at each stage;
- L decreases of 0.5 meters at each stage.

In the next chapter, the covered trajectories realized with these parameters are shown.

7. Results

Having already explained in chapter 4 the creation of the model and the code adopted in the simulation, the plots and results attained are shown using the parametrisation in figure 27.

7.1 Drowsy drivers in double lane change

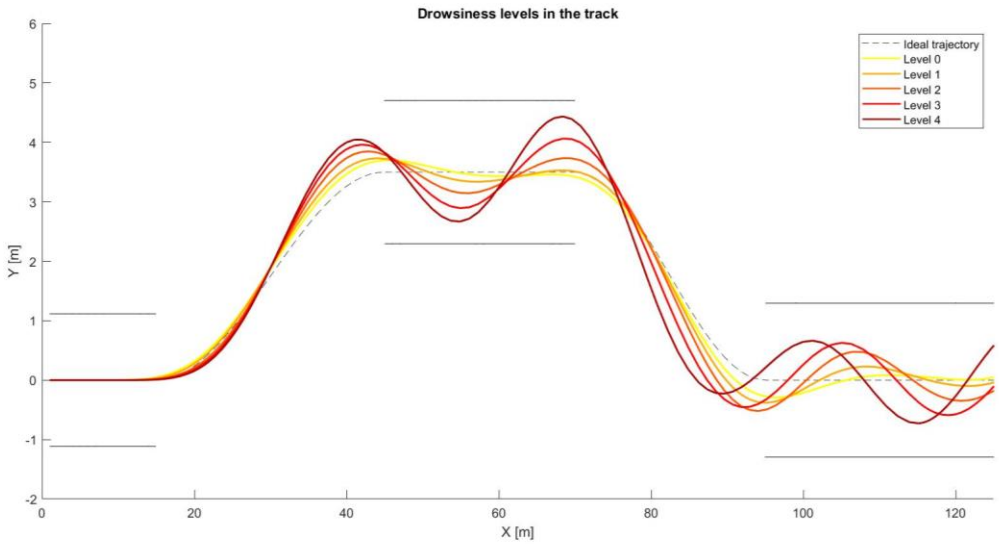

Figure 28: Drowsiness levels in the double lane change manoeuvre

This was the first step of the design phase in which the desired discretization is created. The guideline is to have all the levels inside the lanes of the standardized test in order to avoid to project driver too tired who exit from the road causing a dangerous situation. The yellow colour as clarified in the legend is referred to the alert driver while the dark red is for the more drowsy; in between the intermediate levels. The subdivision has to be done considering pilots able to drive who start to give signs of skidding off. Therefore, also the higher level with larger peaks and

oscillations is always within the lanes with a safety margin; providing a positive result in the stability test of the double lane change manoeuvre.

Even if they are all originated by a predictive driver model, the extremes manifest different behaviour. The vigilant car user has a real predictive trend since the trajectory covered by the centre of mass of the vehicle is in advance with respect to the dashed ideal trajectory. Instead, for what is concerned the more sleepy drivers of level 3 and 4, they behave as not predictive driver as the travelled trajectory is in late with reference to the centreline.

In the plot below, a real width road is inserted to visualise the effective safety margin.

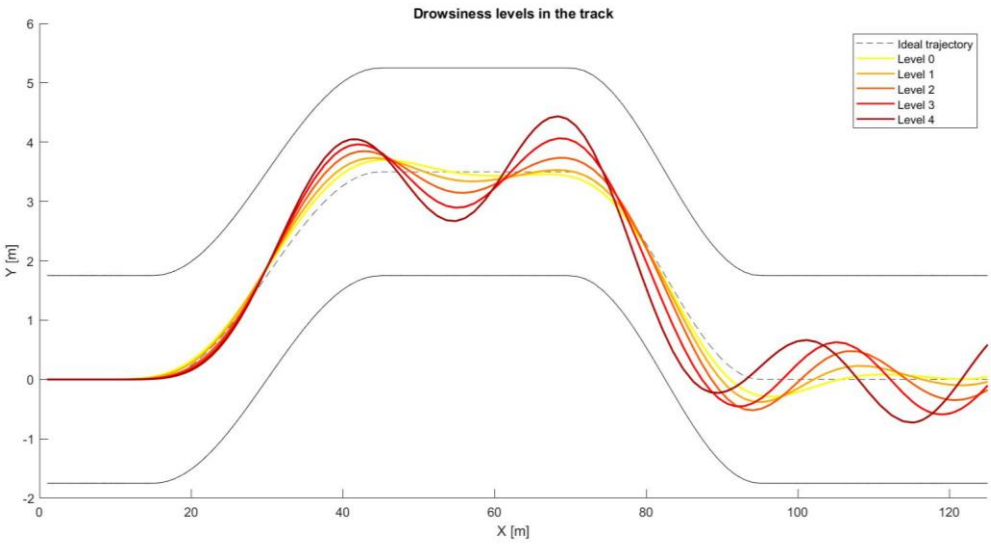

Figure 29: Drowsiness levels in the double lane change manoeuvre in real road

This standardized manoeuvre simulates a real overtaking since the lateral displacement between the two lanes is 3.5 meters so it is suitable for an examination of the real world and the addition of segments in the track.

In according with the variable used in the parametrisation it is important to notice that as anticipated:

- growing the drowsiness level, the peaks and oscillations increase due to the progressive increment of the gains K_p and K_i;
- the merged effect of τ and L, respectively the first one increased gradually with the subdivision and the second one decreased, is to delay the system.

Thus, the outcomes are in agreement with the theory and with the expected results.
Underneath, the real scaled plot in the top view is shown in order to see the current trajectories:

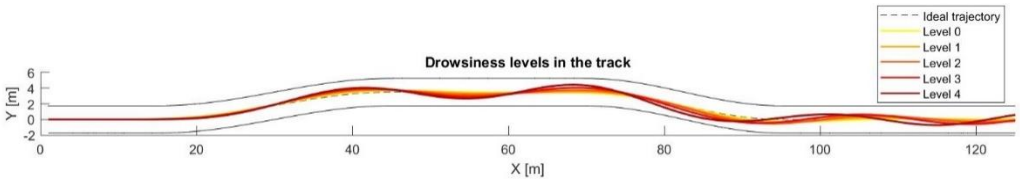

Figure 30: Real double lane change levels in top view

In the top view, the smoothness of the manoeuvre is specified in contrast with the figure 29 used to evidence the differences among the levels.

7.2 Drowsy drivers in open track

Obtaining good results in agreement with what was expected, the same discretization is used in the new invented open track in order to see if the path is followed in the right way or there are signs of decay in a longer road.
Before showing the effect in the route, the graphical application of the predictivity is described. According to what is explained in chapter 6, every drowsy driver model is described by its parameters and in particular, the predictivity implementation is examined in this part.

It is expressed in meters, but converted in time for easier employment so that the input provided to the model is just a shift of the ideal trajectory.

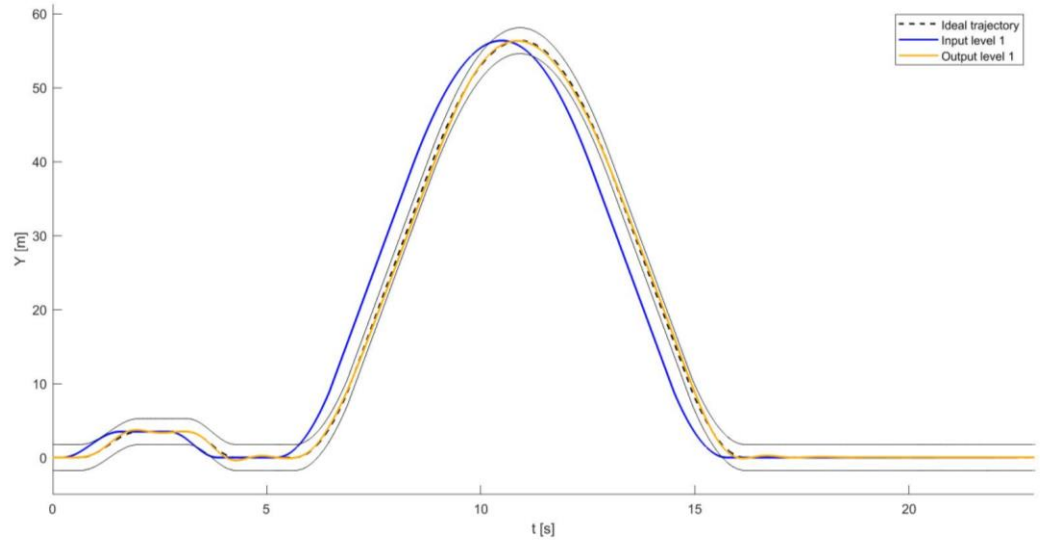

Figure 31:Predictive input

As depicted in the image, in blue, the input has the same shape of the ideal curvature, but anticipated. In function of the relative number for its level, being the speed constant, the time shift is clearly computed as the ratio between the space and the rate.

Clarified the pragmatic ruse for the predictivity, the results relative to the open track are exhibited.

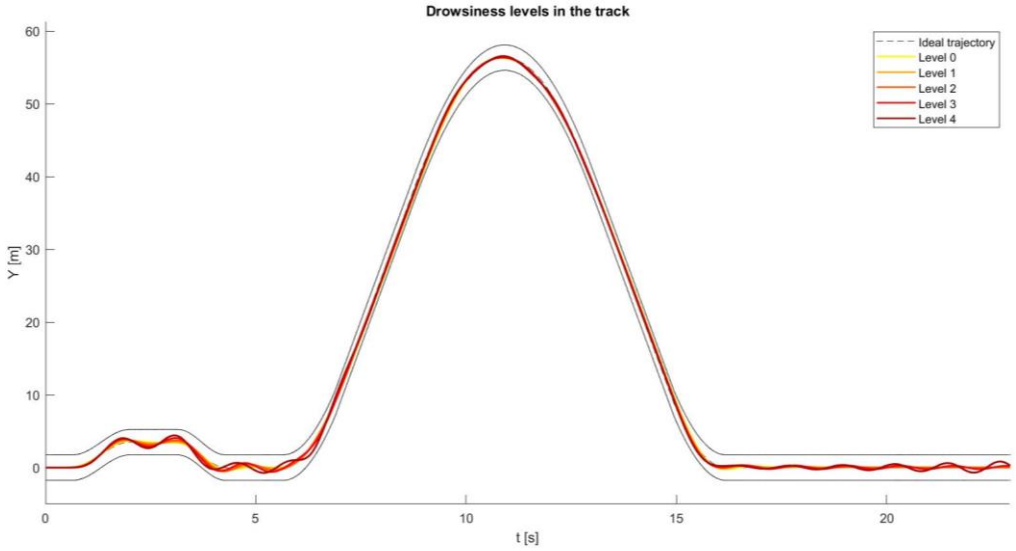

Figure 322: Drowsiness levels in open track vs time

As always, for better visibility, a not scaled plot is presented. First of all, it is apparent that no critical situations occur during travel so neither the last level goes off the road. Approximately all the subdivisions stay in proximity of the centreline. During the last straight segment, it is noticeable that after almost 17 seconds from the start, driving always at the same drowsiness level create an unstable condition. Clearly, the identical situation is visible plotting versus the longitudinal distance:

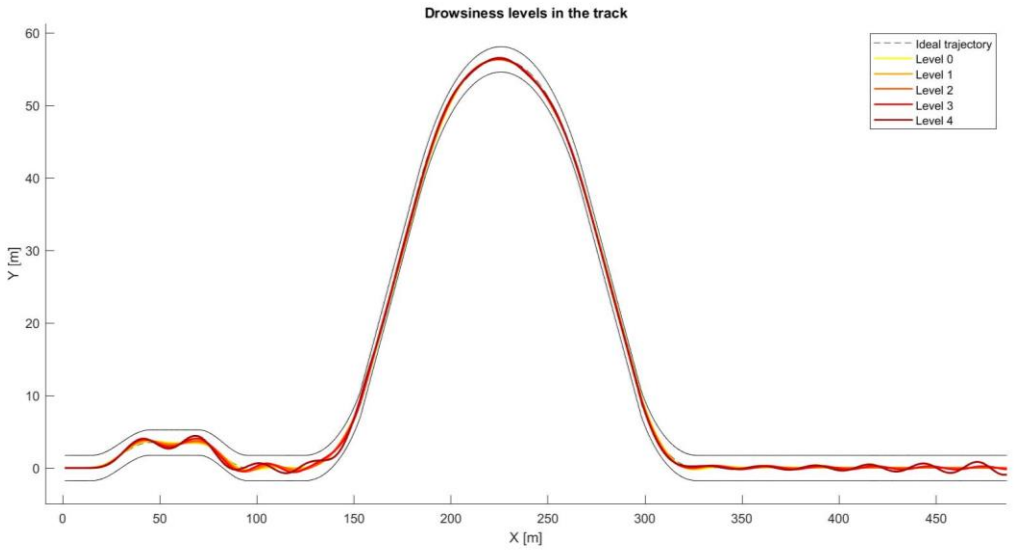

Figure 33: Drowsiness levels in open track

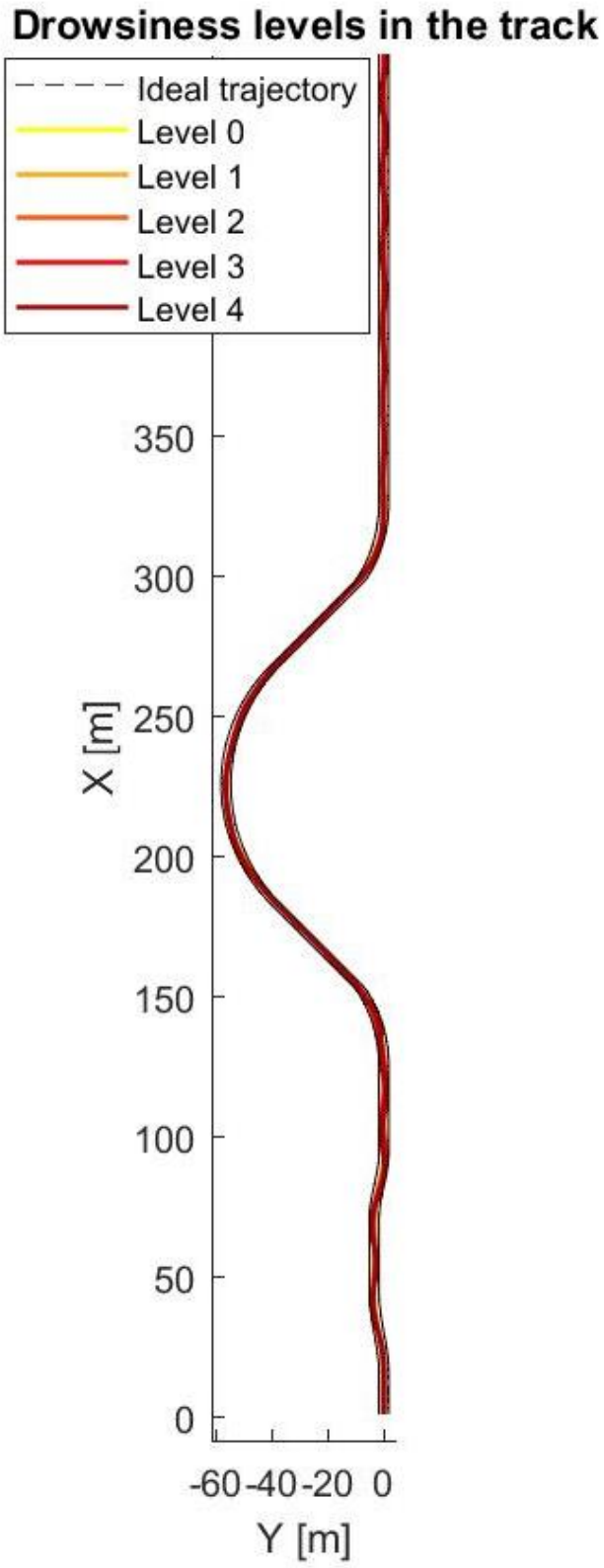

Figure 34: Levels in top view

Also if the discretization is not clear, the fourth level is a little bit more unstable than the others. This behaviour is caused by a fixed design of the parameters that imply unsteadiness in longer trips.

In order to evidence the drivers' behaviour, a brief examination of each road section is proposed:

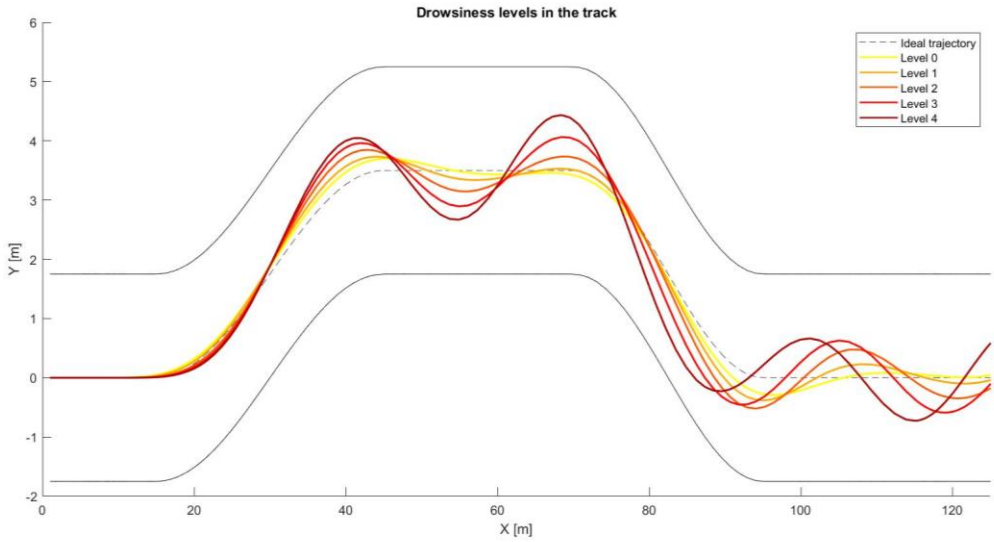

Figure 35: Double lane section

The first part is the one referred to the double lane change thoroughly seen in the dedicated division. The levels are well smoothly discretized with the more vigilant drivers who cut the curves in advance.

Level 0 is the most stable with fewer fluctuations and the fastest response.

After this, the added segments are evaluated excluding the intermediate rectilinear streets in which no significant considerations can be done.

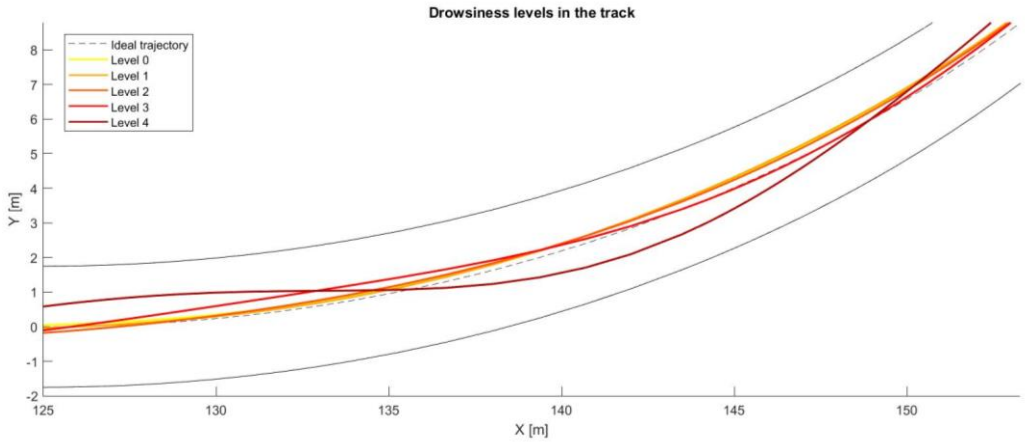

Figure 36: 1st curve to the left

The trajectories performed by the lower levels 0-1-2 are practically coinciding and they are always following the centreline with a small advance. The level 3 has a little delay whereas, the last stage generates an unstable path with many vacillations before reaching the middle of the road before the straight. Nevertheless, it is always within the lanes with a decent safety allowance. This trend suggests a real drowsy driver since the numbers of the so called zero crossing is higher than the alert car users. Zero crossing means the frequency related to the oscillations with respect to the centreline. Every time the vehicle switches the side of the road, delimitated by the dashed line, the counter increases.

Neglecting the straight road, the ninety degrees curve is shown:

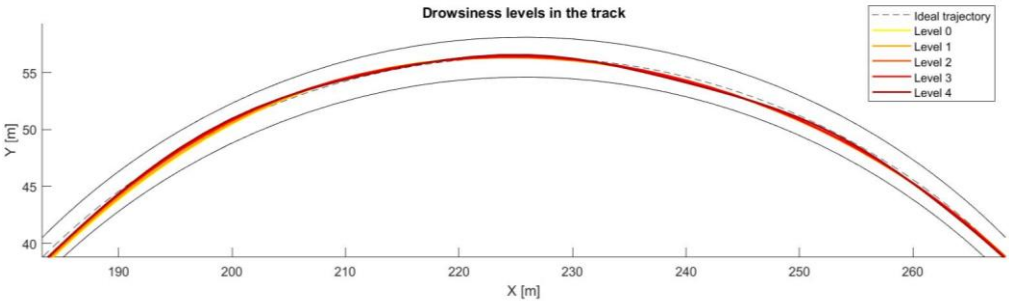

Figure 37: 2nd curve to the right

Yet again, the alert driver, due to the highest predictivity and in general the trade-off achieved with all the parameters, is driving obtaining the finest course. In fact, it is in advance and then develops the arc, tangent to the middle of the street. Also, the other stages are steady but levels 3 and 4 show fluctuations around the centreline of small amplitude.

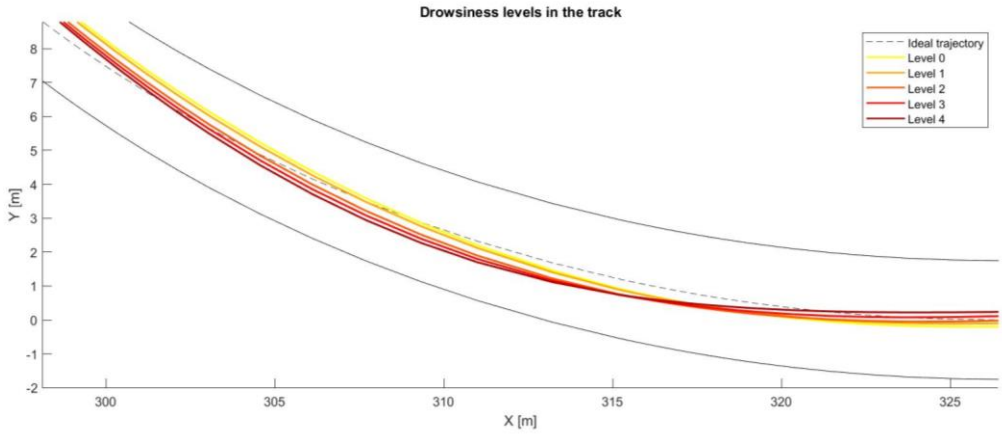

Figure 38: 3rd curve to the right

The last curve of 45 degrees is accomplished and the same behaviour is attained. As expected by the theory, up to now, the lower levels are more stable and the distinctive feature is the advance and the cut of the curve. The more drowsy drivers denote a lag with movements less smooth. It is important to remember that the lines are representing the travelled path of the mass centre; so including also the volume of the vehicle, the oscillations extensively reduce the safety distance from the lateral boundaries.

The last straight is displayed:

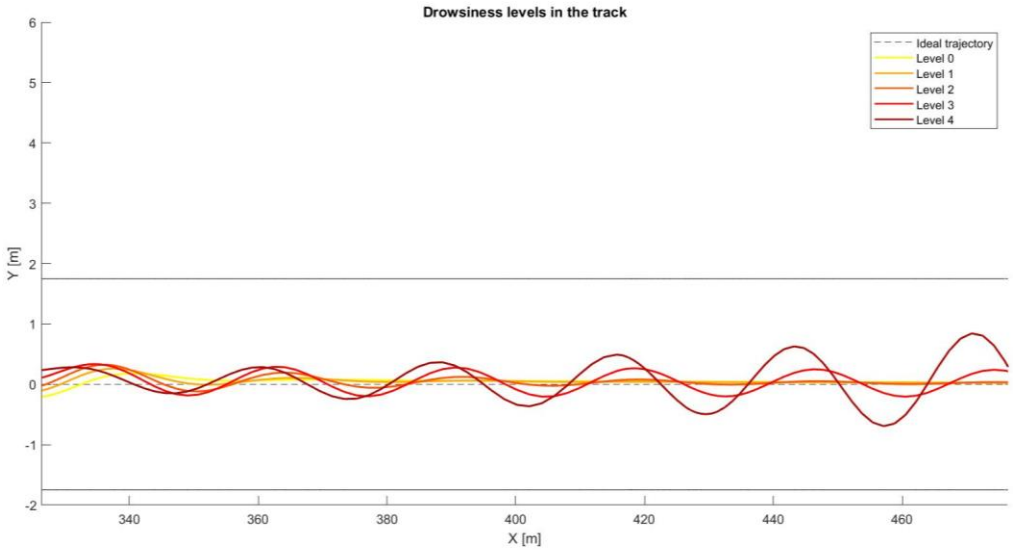

Figure 39: last straight section

Here, strong oscillations arise. Levels 0-1-2 give perfect results since they are able to keep the stability also when a straight road has to be travelled, as it was expected for alert drivers, while stages 3 and 4 start to fluctuate further and further. This, after verifying it was not due to mathematical problems, is attributed to a real interpretation of the drowsy driver. Indeed, it is caused by the coefficients that are fixed and so the model always corrects the current position with the same gains. Physically, it represents the situation in which the drowsy driver, after a quite long stand still, acts with an abrupt correction. The error arises and correcting always with the same gain, the consequence is the one plotted in the picture 38.

8. Conclusions

The development of driving aids to reduce dangerous accidents is an increasingly topical issue. Specifically for the drowsiness, the focus is to recognize the degree of fatigue of the car user to warn him in case of clear symptoms of tiredness.

This document deals with the study and simulation of different drowsiness levels of drivers of motor vehicles during travel.

In the beginning, an overall view of the existing techniques for identifying drowsiness is presented. The detection methods have been divided based on the monitored object. When the driver is monitored, physiological measurements like brain activity, heart rate and muscle vibration or facial identification, managed by artificial intelligence can be used. The latter one examines eyes, eyelids, head movements and expressions like frequent yawning using cameras.

Physiological measurements allow the best accuracy, but they are often intrusive and so impractical due to the discomfort.

When the supervised object is the vehicle, the steering wheel angle, computed by a sensor, is analysed. Based on the frequency of the changes and other parameters, the software calculates the driver's level of fatigue in a complete, non-invasive way. Due to this and according to the commercial investigation, the steering wheel pattern has been chosen for this project since it is the most widespread system.

Then the theoretical outlines referred to the adopted vehicle model and the driver have been provided in order to define the assumptions and so the simplifications taken into account. In the end, the drowsy driver is represented by a PI controller, in which the gains simulate the steering wheel actions, by a driver delay to emulate the time response and by the predictivity so that the human visual effect is involved. To achieve the purpose of this project and to replicate different levels of a drowsy driver, a track was necessary to analyse the different trajectories. For this reason, the standardized ISO double lane change manoeuvre has been chosen

to design the different stages. The idea was to create a smooth discretization between the levels in which also the worst condition was within the lane to avoid simulating very critical and dangerous situations as off-road crashes. Once the right combination of all the variables that give the desired behaviour has been defined, a longer open track has been designed to test the drowsy drivers in a distinct environment. All the results are satisfactory since no dangerous circumstances have been monitored unless for level 4 in which the oscillations generated by the driver, during the last straight, arise obtaining an unstable path. Nevertheless, in general the trends of the levels are the ones expected, in line with the theoretical concepts of the tuning: the attentive driver categorized as level 0 is the most stable cutting the curves following the ideal trajectory in advance; the most sleepy driver described by level 4 is the most unstable expressing fluctuations and a bit of delay in the covered path. Also, the physical representation is well described and reflects the results: when looking at the trajectories, the steering outputs in fatigued drivers are shown to have fewer micro corrections and more macro-corrections in a larger period.

8.1 Future works

The designed levels can be considered a good representation of drowsy drivers and from this, mathematical models can be implemented in order to enlarge the study. As different studies have shown, analysing the steering behaviour, the travelled trajectory and adopting a statistical approach, an observer, for example, can be added to the model to predict a dangerous situation and warn the driver to take a break in time.

This could be done considering:

- the long standstill, so the time in which the driver is not correcting the trajectory either with micro corrections;
- the amplitude of the corrections directly on the steering wheel inserting in the computation a steering transmission ratio;

- the zero crossing effect, so basically the frequency of oscillations, from left to right and vice versa, referred to the centreline of the lane and;
- the lane monitoring, so measuring the relative distance concerning the right and left lane and evaluate eventual skidding off.

Another approach could be to build on a parallel system that detects drowsiness using different methods like facial recognition, pedal pressure analysis to cross-reference utilizing artificial intelligence and physical measurement as a reference if possible.

Acknowledgements

Firstly, I would like to be grateful to my company tutor, Eng. Alberto Bertone for his patient, his teachings and his essential support during each phase of this thesis. It was a good team work during all these months. I cannot forget my special supervisor La Misul who is really sunny and tough at the same time. With her advice she helps you to focus on the important things giving wise lessons for the job environment. Her professionalism was the reason I wanted her to be my supervisor.

Then, I would like to thank Teoresi Group to have given the opportunity to accomplish this thesis project in the headquarter despite the pandemic problem. It is a pleasure work with them.

An obvious and important thanks is for my family: my mum, my father and my brother; they are always with me bearing me especially in this final, not easy, period. A recognition to all my aunties, uncles, cousins and my grandmother, they gave always a strong support with all their words.

A proper thank you is for all my friends, too many to mention, from Pinerolo and Torino with whom I share my free times and entertainment. A particular thanks is for Stanuccio who was the first one I met the first day of all my academic career.

Last but not least, the special thanks is for my love Giulia who has always been close to me supporting me and advising me all these years. If I have finished this master degree it is surely thanks to her.

Bibliography

[1] T. Ranney, E. Mazzae, R. Garrott, and M. Goodman, “NHTSA driver distraction research: Past, present, and future,” *USDOT, Natl. Highw. Traffic Saf. Adm.*, pp. 1–11, 2000, [Online]. Available: http://www-nrd.nhtsa.dot.gov/departments/Human Factors/driver-distraction/PDF/233.PDF.

[2] E. T. S. C. Etsc, *The Role of Driver Fatigue in Commercial Road Transport Crashes*. 2001.

[3] A. W. MacLean, D. R. T. Davies, and K. Thiele, “The hazards and prevention of driving while sleepy.,” *Sleep Med. Rev.*, vol. 7, no. 6, pp. 507–521, Dec. 2003, doi: 10.1016/s1087-0792(03)90004-9.

[4] P. Thiffault and J. Bergeron, “Fatigue and individual differences in monotonous simulated driving,” *Pers. Individ. Dif.*, vol. 34, pp. 159–176, Jan. 2003, doi: 10.1016/S0191-8869(02)00119-8.

[5] Q. Ji and X. Yang, “Real-time eye, gaze, and face pose tracking for monitoring driver vigilance,” *Real-Time Imaging*, vol. 8, no. 5, pp. 357–377, 2002, doi: 10.1006/rtim.2002.0279.

[6] J. F. May and C. L. Baldwin, “Driver fatigue: The importance of identifying causal factors of fatigue when considering detection and countermeasure technologies,” *Transp. Res. Part F Traffic Psychol. Behav.*, vol. 12, no. 3, pp. 218–224, 2009, doi: 10.1016/j.trf.2008.11.005.

[7] B. T. Jap, S. Lal, P. Fischer, and E. Bekiaris, “Using EEG spectral components to assess algorithms for detecting fatigue,” *Expert Syst. Appl.*, vol. 36, no. 2 PART 1, pp. 2352–2359, 2009, doi: 10.1016/j.eswa.2007.12.043.

[8] S. K. L. Lal, A. Craig, P. Boord, L. Kirkup, and H. Nguyen, “Development of an algorithm for an EEG-based driver fatigue countermeasure,” *J. Safety Res.*, vol. 34, no. 3, pp. 321–328, Aug. 2003, doi: 10.1016/S0022-4375(03)00027-6.

[9] G. Cario, “Metodi e algoritmi per il riconoscimento del livello di distrazione e affaticamento nella guida di autoveicoli.”

[10] T. Hayami, K. Matsunaga, K. Shidoji, and Y. Matsuki, “Detecting drowsiness while driving by measuring eye movement- A pilot study,” in *IEEE Conference on*

Intelligent Transportation Systems, Proceedings, ITSC, Jan. 2002, vol. 2002-January, pp. 156–161, doi: 10.1109/ITSC.2002.1041206.

[11] S. Yang, J. Xi, and W. Wang, "Driver drowsiness detection through a vehicle's active probe action," *2019 IEEE 2nd Connect. Autom. Veh. Symp. CAVS 2019 - Proc.*, no. 61703041, 2019, doi: 10.1109/CAVS.2019.8887773.

[12] K. H. Noh, C. K. Rah, Y. S. Yoon, and K. S. Yi, "Experimental approach to developing human driver models considering driver's human factors," *Int. J. Automot. Technol.*, vol. 15, no. 4, pp. 655–666, May 2014, doi: 10.1007/s12239-014-0068-9.

[13] J. Ishio, H. Ichikawa, Y. Kano, and M. Abe, "Vehicle-handling quality evaluation through model-based driver steering behaviour," in *Vehicle System Dynamics*, 2008, vol. 46, no. SUPPL.1, pp. 549–560, doi: 10.1080/00423110801993169.

[14] N. Mehrabi, R. S. Razavian, and J. McPhee, "A Physics-Based Musculoskeletal Driver Model to Study Steering Tasks," *J. Comput. Nonlinear Dyn.*, vol. 10, no. 2, pp. 1–8, 2015, doi: 10.1115/1.4027333.

[15] F. Friedrichs and B. Yang, "Drowsiness monitoring by steering and lane data based features under real driving conditions," *Eur. Signal Process. Conf.*, pp. 209–213, 2010.

[16] A. Mortazavi, A. Eskandarian, and R. A. Sayed, "Effect of drowsiness on driving performance variables of commercial vehicle drivers," *Int. J. Automot. Technol.*, vol. 10, no. 3, pp. 391–404, Jun. 2009, doi: 10.1007/s12239-009-0045-x.

[17] R. B. Gmbh, "Chassis Systems Control Driver Drowsiness Detection," 2010.

[18] G. Genta and L. Morello, *Volume 2: System Design*. 2009.

[19] M. M. Artamonov, M. D., Ilarionov, V. A., & Morin, *Motor vehicles: Fundamentals and design.* Moscow: Mir Publishers., 1976.

[20] R. Rqajamqni, *Vehicle Dynamics and Control*, 2006th ed. New York: Springer.

[21] G. Genta, *Motor vehicle dynamics*. Torino: World Scientific, 2006.

[22] T. Lee, J. Kang, K. Yi, and K. Noh, "An investigation on the integrated human driver model for closed-loop simulation of intelligent safety systems," *J. Mech. Sci. Technol.*, vol. 24, no. 3, pp. 761–767, 2010, doi: 10.1007/s12206-010-0202-1.

[23] A. Li, H. Jiang, J. Zhou, and X. Zhou, "Implementation of Human-Like Driver Model Based on Recurrent Neural Networks," *IEEE Access*, vol. 7, pp. 98094–98106, 2019, doi: 10.1109/ACCESS.2019.2930873.

[24] X. Zhou, H. Jiang, A. Li, and S. Ma, “A New Single Point Preview-Based Human-Like Driver Model on Urban Curved Roads,” *IEEE Access*, vol. 8, pp. 107452–107464, 2020, doi: 10.1109/ACCESS.2020.3001208.

[25] P.G.Perotto, *Sistemi di automazione*. Torino: UTET, 1970.

[26] A. E.-N. G.F. Franklin, J.D. Powell, *Feedback Control of Dynamic Systems*. Prentice Hall, 2009.

[27] Araki M, “PID CONTROL.”

[28] K. H. Ang, G. C. Chong, and Y. Li, “PID control system analysis, design, and technology,” *IEEE Trans. Control Syst. Technol.*, vol. 13, no. 4, p. 559, 2005, doi: 10.1109/TCST.2005.847331.

Sitography

Figure 1: Drowsiness detection
https://www.bosch-mobility-solutions.com/en/solutions/assistance-systems/driver-drowsiness-detection/

Figure 2: Physiological measurement
https://www.slideshare.net/InsideScientific/integrating-eye-tracking-data-with-physiological-measurements

Figure 3: Facial recognition
https://readwrite.com/2020/01/19/facial-recognition-shaping-the-future-of-identity-verification-market/

Figure 4: Lane monitoring
https://www.extremetech.com/extreme/165320-what-is-lane-departure-warning-and-how-does-it-work

Figure 6: Attention assist
https://media.daimler.com/marsMediaSite/en/instance/ko/ATTENTION-ASSIST-Drowsiness-detection-system-warns-drivers-to-prevent-them-falling-asleep-momentarily.xhtml?oid=9361586

Bosch: https://www.bosch-mobility-solutions.com/en/products-and-services/passenger-cars-and-light-commercial-vehicles/driver-assistance-systems/driver-drowsiness-detection/

https://www.bosch-mobility-solutions.com/en/products-and-services/passenger-cars-and-light-commercial-vehicles/interior-and-body-systems/interior-monitoring-systems/

Driver Attention Monitoring – DS: https://it-media.dsautomobiles.com/it/ds-7-crossback-sicurezza-ai-massimi-livelli-con-il-ds-driver-attention-monitoring

Driver Alert – FORD: https://www.haynesford.co.uk/Tech-Ford-driver-alert

Driver Attention Monitoring – HONDA: https://www.hondainfocenter.com/2021/CR-V/Feature-Guide/Interior-Features/Driver-Attention-Monitor/

Driver Attention Alert – HYUNDAI: https://www.hyundai.com/au/en/why-hyundai/autonomous-driving/safety#:~:text=local%20Hyundai%20dealer.-,Driver%20Attention%20Alert%20(DAA).,driver%20to%20take%20a%20break

Driver Monitor System - JAGUAR LAND ROVER: https://www.landrover.ca/en/explore-land-rover/news/jlr-new-driver-monitor-system.htm

Driver Attention Warning - KIA: http://www.kisouman.com/driver_attention_warning_daw_system-3332.html

Attention Assist - MERCEDES: https://mbenz.it/mercedes-attention-assist-compie-10-anni/16413/

Driver Attention Alert – NISSAN: https://usa.nissannews.com/en-US/releases/nissan-s-driver-attention-alert-helps-detect-erratic-driving-caused-by-drowsiness-and-inattention

Fatigue Detection Warning - RENAULT: http://www.rkoleos.com/70/fatigue_detection_warning.html

EyeSight Driver Assist – SUBARU: https://www.subaru.com/engineering/eyesight.html

iBuzz Fatigue Alert – SKODA : https://drivetribe.com/p/skoda-safety-ibuzz-fatigue-alert-f43lX1BbTT2Mn-XhfC26jg?iid=KMjPkkPHTOGBDutm73FJYQ

Fatigue Detection System – AUDI and VW: https://autoblog.amag.ch/it/come-funziona-il-sistema-di-rilevamento-della-stanchezza-alla-guida/#:~:text=Nei%20modelli%20VW%20e%20Audi,di%20guida%20di%2015%20minuti

Driver Attention Assist – BMW: https://www.autonews.com/article/20180927/OEM04/180929798/at-bmw-a-camera-can-now-monitor-x5-driver-attention

Driver Alert Control – VOLVO: https://www.volvocars.com/it/support/manuals/xc40/2018w46/supporto-al-conducente/driver-alert-control/driver-alert-control

Driver Drowsiness Alert – OPEL: https://gmauthority.com/blog/2017/08/driver-drowsiness-alert-highlights-opel-grandland-x-safety-features/

Driver Attention Alert – PEUGEOT: https://www.peugeot.co.uk/technology/latest-peugeot-technology/intelligent-driver-aids/

Driver Attention Assist – ALFA ROMEO: https://www.alfaromeo.it/sistemi-guida-assistita-adas/driver-attention-assist?adobe_mc_ref=

Bentley: https://kommunikasjon.ntb.no/pressemelding/panasonic-develops-drowsiness-control-technology-by-detecting-and-predicting-drivers-level-of-drowsiness?publisherId=90063&releaseId=15669977

Seat: https://fleetservicessummit.co.uk/briefing/seat-experimenting-with-driver-fatigue-detection-tech/

Lexus : https://drivers.lexus.com/lexus-drivers-theme/pdf/LSS+%20Quick%20Guide%20Link.pdf

Appendix A

A.1 Market systems

In this division, there will be recorded all the devices taken into account in the classification of the market trend inside the chapter 1. The list can be considered updated up to the year 2018.

- For the section steering monitoring and lane monitoring:

  Driver Attention Monitor – HONDA

  Driver Attention Alert – HYUNDAI

  Driver Attention Alert – NISSAN

  Fatigue Detection Warning – RENAULT

  iBuzz Fatigue Alert – SKODA

  Driver Alert Control – VOLVO

  Driver Attention Assist – ALFA ROMEO

  Below, the systems without steering wheel sensor, they compare just the trajectory with respect to the lane;

  Driver Alert – FORD

  Driver Attention Warning – KIA

  Lane Departure Warning System – CITROEN

  Driver Attention Alert – PEUGEOT

  Driver Drowsiness Alert – OPEL

  EyeSight Driver Assist – SUBARU

- For the section driver/eye monitoring and lane monitoring:

  Driver Attention Monitoring – DS

  Drive Monitor System – JAGUAR/LAND ROVER

  Drive Attention Alert – MAZDA

Super Cruise System – CADILLAC

Driver Attention Assist – BMW

Driver Monitoring System – TOYOTA

- For the section steering monitoring, driver/eye monitoring and lane monitoring together with also pedal pressure analysis:

  Attention Assist – MERCEDES

  Fatigue Detection System – AUDI/VW

A.2 Car segment involvement

In this part, the detail of section 1.3.1 is presented. In the table below, the brand analysed for the creation of the figure 7 about the current market trend is shown:

	B	C	D	E	F	J	M	*Type*
DS				✓		✓		1500 €
FORD						✓		
HONDA						✓		
HYUNDAI		✓				✓		
KIA		✓				✓		
MAZDA		✓	✓			✓		
MERCEDES		✓	✓	✓	✓	✓	✓	
NISSAN		✓				✓	✓	
RENAULT						✓	✓	
SKODA	✓	✓	✓			✓		
AUDI	✓	✓	✓	✓	✓	✓	✓	
VW	✓	✓				✓	✓	
BMW		✓	✓	✓	✓	✓	✓	Opt 920 €
VOLVO				✓		✓		Opt 610 €
PEUGEOT		✓	✓			✓		

Again, these considerations are updated up to the year 2018. In the column type, the typology of the system is specified if the car maker offers the device optionally, otherwise no if it is integrated in the list price with other safety systems.

Appendix B

In this appendix, the code referred to the data is submitted.

```
g=9.81;

%% Mass and Jz

m_ns_front=2*35;  % [kg]    unsprung mass front axle
m_ns_rear=2*30;   % [kg]    unsprung mass rear axle
fuel=30;          % [kg]
m_s=1600-m_ns_front-m_ns_rear+fuel;  % [kg]  sprung mass
m=m_s+m_ns_front+m_ns_rear;       % [kg]  total vehicle mass

J_z=1/12*m_s*(1.75^2+3.8^2);  % [kgm^2] jaw moment of
inertia

%% Dimensions

l=2.600;  %  [m]    wheel base

%CG_LOCATION=0.55 Front Weight distribution in percentage
(AsettoCorsa suspension.ini file)

a=l*(1-0.55);  % [m]
b=l-a;         % [m]

%BASEY=-0.15 Distance of CG from the centre of the wheel in
meters.
%Wheel Radius+BASEY=front CoG.  FWR RADIUS=0.30815
%Wheel Radius+BASEY=rear CoG.   RWR RADIUS=0.30815
%Actual CG height =(FWR+FBasey)+(RWR+Rbasey))/CG_LOCATION

%hG=0.6; % [m]  height of the centre of gravity

t=1.610; % [m]  wheel track front and rear
hRC=0.4; % [m]  roll centre height
ss=1.15; % [m]  spring span

%% Vertical load

% front wheel vertical force [N]
Fz1=(m_s*g*(l-a)/l+m_ns_front*g)/2;

% rear wheel vertical force  [N]
Fz2=(m_s*g*a/l+m_ns_rear*g)/2;
```

```
%% Cornering stiffness and self-aligning moment

%  [N/rad] front axle lateral stiffness
C_1=2*(50000/2700)*Fz1;     % mu1*fz1

%  [N/rad] rear axle lateral stiffness
C_2=2*(50000/2700)*Fz2;     % mu2*fz2

%  [Nm/rad] front axle stiffness of the self-aligning moment
M_z_alpha1=2*(4000/2700)*Fz1;

%  [Nm/rad] rear axle stiffness of the self-aligning moment
M_z_alpha2=2*(4000/2700)*Fz2;

%% Suspension stiffnesses

Ks_front= 55000; % [N/m]
Ks_rear=65000;   % [N/m]
K_antirollbar_f=18000/360;       % [Nm/deg]
K_antirollbar_r=4500/360;        % [Nm/deg]

Psi_f=((ss^2*Ks_front/1375)+K_antirollbar_f)*180/pi;
% [Nm/rad]
Psi_r=((ss^2*Ks_rear/1375)+K_antirollbar_r)*180/pi;
% [Nm/rad]

%% Aerodynamics

Cx=0.35;
rho=1.225;          % [kg/m^3]  air density
S=2.5;              % [m^2]     projection area
C_beta=-2.31;       % lateral force coefficient
C_Mz=-0.31;         % aerodynamic coefficient about z axis
```